Persoonia 55, 2025: 159–201
https://www.persoonia.org

RESEARCH ARTICLE

ISSN (Online) 1878-9080
https://doi.org/10.3114/persoonia.2025.55.05

Polyphasic taxonomy and chemical diversity of *Annulohypoxylon* (*Ascomycota*, *Hypoxylaceae*): New species from China's tropical forest

Q.R. Li[1,2#], Y.H. Pi[1,2], E. Charria-Girón[3,4#], K. Habib[1,5#], H.M. Hu[1], S. Wongkanoun[6,7], M. Stadler[3,4*], L.L. Liu[1,2], X.C. Shen[2,8], J.C. Kang[9*]

[1]State Key Laboratory of Discovery and Utilization of Functional Components in Traditional Chinese Medicine & School of Pharmaceutical Sciences, Guizhou Medical University, Guian New District, Guizhou 550004, China
[2]The High Efficacy Application of Natural Medicinal Resources Engineering Centre of Guizhou Province (The Key Laboratory of Optimal Utilization of Natural Medicine Resources), School of Pharmaceutical Sciences, Guizhou Medical University, Gui'an New District, 561113, P.R. China
[3]Department of Microbial Drugs, Helmholtz Centre for Infection Research GmbH (HZI), German Centre for Infection Research Association (DZIF), partner site Hannover-Braunschweig, Inhoffenstraße 7, 38124 Braunschweig, Germany
[4]Institute of Microbiology, Technische Universität Braunschweig, Spielmannstraße 7, 38106 Braunschweig, Germany
[5]Department of Botany, Khushal Khan Khattak University, Karak, KP, Pakistan
[6]Department of Biochemistry and Microbiology, Center of Excellence for DNA Barcoding of Thai Medicinal Plants, Faculty of Pharmaceutical Sciences, Chulalongkorn University, Bangkok 10330, Thailand
[7]National Biobank of Thailand (NBT), National Center for Genetic Engineering and Biotechnology (BIOTEC), 111 Thailand Science Park, Phahonyothin Road, Khlong Nueng, Khlong Luang, Pathum Thani 12120, Thailand
[8]Key Laboratory of Environmental Pollution Monitoring and Disease Control, Ministry of Education, School of Basic Medical Sciences, Guizhou Medical University, Gui'an New District, 561113, P.R. China
[9]Engineering and Research Centre for Southwest Bio–Pharmaceutical, Resources of National Education Ministry of China, Guizhou University, Guiyang, 561113, P.R. China

[#]These authors contributed equally
[*]Corresponding authors: J.C. Kang, jckang@gzu.edu.cn; M. Stadler, marc.stadler@helmholtz-hzi.de

Key words:
fungal diversity
metabolomics
new taxa
taxonomy
tropical mycology
Xylariales

Abstract: As part of an ongoing inventory of *Ascomycota* in China, we examined species of the genus *Annulohypoxylon* collected from tropical forests. Through a comprehensive analysis encompassing phylogenetic, chemotaxonomic, and morphological data, we provide descriptions, illustrations, and diagnostic keys for 17 species. Among these, 14 are newly described species, while three represent new records for the studied region. In addition, evidence from phylogenetic, chemotaxonomic, and morphological analyses prompted the re-examination of the taxonomic status of *Rostrohypoxylon*, resulting in it being reduced to synonymy under *Annulohypoxylon*. This study underscores the large yet underexplored diversity of *Hypoxylaceae* in China's tropical forests. While numerous *Xylariales* fungi have been documented in these regions, the diversity within the family *Hypoxylaceae* remains largely unexplored, leaving significant potential for further discoveries. Moreover, metabolomic profiling using ultrahigh performance liquid chromatography coupled to diode array detection and ion mobility tandem mass spectrometry (UHPLC-DAD-IMS-MS/MS) revealed a hidden diversity of stromatal metabolites among the studied taxa, independent of their taxonomic relationships.

Citation: Li QR, Pi YH, Charria-Girón E, Habib K, Hu HM, Wongkanoun S, Stadler M, Liu LL, Shen XC, Kang JC (2025). Polyphasic taxonomy and chemical diversity of *Annulohypoxylon* (*Ascomycota*, *Hypoxylaceae*): New species from China's tropical forest *Persoonia* **55**: 159–201. doi: 10.3114/persoonia.2025.55.05
Received: 19 September 2024; **Accepted:** 17 June 2025; **Effectively published online:** 5 September 2025.
Corresponding editor: P.W. Crous

INTRODUCTION

The most recent classification of the class *Sordariomycetes* by Hyde *et al*. (2024) recognizes 19 genera within the family *Hypoxylaceae*, i.e., *Annulohypoxylon*, *Chlorostroma*, *Daldinia*, *Durotheca*, *Entonaema*, *Hypomontagnella*, *Hypoxylon*, *Jackrogersella*, *Natonodosa*, *Phylacia*, *Pyrenomyxa*, *Pyrenopolyporus*, *Rhopalostroma*, *Rostrohypoxylon*, *Ruwenzoria*, *Thamnomyces*, *Theissenia* and *Thuemenella*. Since then, one new genus, *Parahypoxylon*, was introduced (Cedeño-Sanchez *et al.* 2023).

Another genus, *Anthocanalis*, was eventually erected in the *Hypoxylaceae*, but since the DNA sequences of the ex-type strain (generated for four loci) proved to be absolutely identical with those of *Daldinia eschscholtzii* and the morphological features of the sexual morph were absolutely not in accordance with any other taxon in the family, this culture evidently constituted a contaminant (Hyde *et al*. 2020).

© 2025 Westerdijk Fungal Biodiversity Institute

You are free to share - to copy, distribute and transmit the work, under the following conditions:
Attribution: You must attribute the work in the manner specified by the author or licensor (but not in any way that suggests that they endorse you or your use of the work).
Non-commercial: You may not use this work for commercial purposes.
No derivative works: You may not alter, transform, or build upon this work.
For any reuse or distribution, you must make clear to others the license terms of this work, which can be found at https://creativecommons.org/licenses/by-nc-nd/4.0/. Any of the above conditions can be waived if you get permission from the copyright holder. Nothing in this license impairs or restricts the author's moral rights.

The strain is unfortunately not alive anymore. Therefore, the genus should be regarded as invalid and was also deleted from the list of valid *Hypoxylaceae* genera in the last Outline of Fungi.

Annulohypoxylon was previously classified within the genus *Hypoxylon*, specifically under the section *Annulata*, distinguished from the section *Hypoxylon* by the presence of an annular ring in the ostiole (Ju & Rogers 1996). Hsieh *et al.* (2005) established the section *Annulata* as a distinct genus, *Annulohypoxylon*, based on the analysis of *β-tubulin* and actin sequences. Concurrently, Quang *et al*. (2005) had already identified the first cohaerin type azaphilones that deviated from the typical mitorubrin and daldinin type azaphilones that are more common in *Hypoxylon*. They also identified truncatone and daldinone A as salient chemotaxonomic markers that are widespread in what is now called *Annulohypoxylon*.

Subsequently, different varieties within the genus were resolved to species level using evidence from phylogenetic, chemotaxonomic, and morphological data (Kuhnert *et al.* 2017). While this led to several new combinations and the establishment of a dichotomous key for the genus, the monophyletic lineage represented by the *A. cohaerens*/*multiforme* group could not be segregated, as their type material was not available during that study. Nevertheless, Wendt *et al*. (2018) finally provided an extensive multigene phylogeny of the *Xylariaceae* using the internal transcribed spacer region of the ribosomal DNA (ITS), the large subunit of the ribosomal DNA (LSU), the second largest subunit of the RNA polymerase II (*rpb2*), and beta-tubulin (*TUB2*) as genetic markers. Their analysis led to the segregation of the genus *Jackrogersella* from *Annulohypoxylon*. They delimited the concept of the genus *Annulohypoxylon* to species with conspicuous ostiolar discs and stromatal pigments predominantly consisting of naphthol derivatives (binaphthalene-tetrol, truncatone A, and daldinol A) or truncaquinones while azaphilones are absent (Sir *et al.* 2018) (Fig. 1). *Jackrogersella* closely resembles *Annulohypoxylon*, but the former differs in containing cohaerin/multiformin type azaphilones as predominant stromatal pigments.

In fact, the secondary metabolites produced by *Annulohypoxylon* spp. display a variety of biological effects with therapeutic potential. For instance, hypoxylonol C-like compounds promote insulin production via the activation of the PI3K/Akt and PDX-1 pathways (Lee *et al.* 2019). Similarly, *A. stygium* produces secondary metabolites with photoprotective properties and devoid of cytotoxic properties (Maciel *et al.* 2018). Despite the findings of promising chemical scaffolds from species of this genus such as N-acetylglucosamine substituted brasilanes, the rare macrolide-like polyketide hypoxylide, or the gymnomitrane-type sesquiterpenes xylariacinols and emericellins, the chemical diversity harboured by these fungi is still uncharted (Liu *et al.* 2018, Feng *et al.* 2020, Gan *et al.* 2023). Currently, *Annulohypoxylon* encompasses approximately 60 species (Wijayawardene *et al*. 2022), mainly reported from tropical and subtropical regions, commonly associated

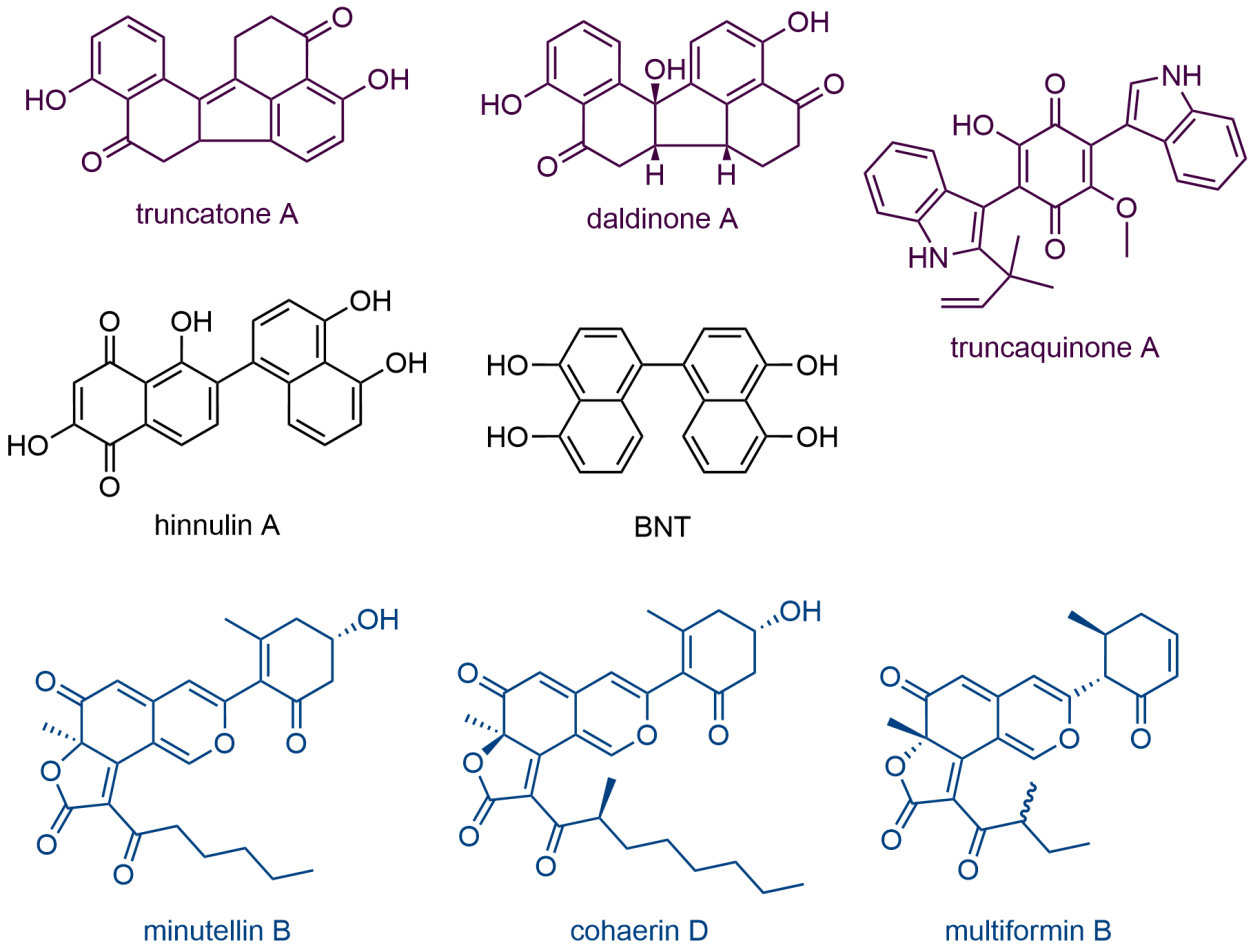

Fig. 1. Chemical structures of secondary metabolites found in the stromata of *Annulohypoxylon* and/or *Jackrogersella* species. In purple and blue are coloured metabolites solely found in *Annulohypoxylon* and *Jackrogersella* spp. respectively, while compounds in black are common to both genera.

with dicotyledonous wood (Hsieh *et al.* 2005, Fournier & Lechat 2016, Kuhnert *et al.* 2017). Some species within this genus have been linked to canker diseases, underscoring their broader ecological impact (Fournier & Lechat 2016, Kuhnert *et al.* 2017). They are also frequently identified as endophytes in seed plants (Ikeda *et al.* 2014). The present study focuses on the exploration of the diversity within the *Hypoxylaceae* in China. Our findings reveal a rich diversity of *Annulohypoxylon*, including 14 newly identified species and document new geographical findings of *Annulohypoxylon* in China.

MATERIALS AND METHODS

Sample collection and storage

The fungal specimens were collected during surveys conducted in the tropical and subtropical regions of China during 2020 and 2021, with all relevant habitat information recorded in a detailed manner. Specimens were photographed using a Canon G15 camera (Canon Corporation, Tokyo, Japan). They were then placed in paper bags and transported for further examination. To remove excess humidity, they were dried using a portable fan dryer. The dried specimens were carefully labelled and stored in an ultra-low freezer at -80 °C for 1 wk after isolation to eliminate any insects and their eggs. Afterwards, the specimens were subjected to morphological analysis. All specimens were deposited at the herbarium of Guizhou Medical University (GMB) and the Herbarium of Cryptogams, Kunming Institute of Botany, Chinese Academy of Sciences (KUN-HKAS). Living cultures were deposited at the Guizhou Medical University Culture Collection (GMBC). All scientific names of fungi follow the entries in MycoBank and Index Fungorum, hence no authorities and years of publications are given in the text apart from the taxonomic entries. Colours and codes were determined following Rayner (1970).

Isolation and morphological characterization

Macroscopic characteristics were examined under an Olympus SZ61 stereomicroscope (Olympus Corp., Japan) and photographed with a Canon 700D digital camera (Canon Inc., Tokyo, Japan). The morphological features were studied as described by Long *et al.* (2019). The samples were mounted in water for microscopic examination, and Melzer's reagent was added to assess the amyloid reaction of the ascal apical apparatus. The Tarosoft (R) Image Framework (v. 0.9.7) and Adobe Photoshop CS6 software (Adobe Systems Inc., USA) were used for measuring and processing images. Axenic cultures were obtained from single spores or tissues as described by Senanayake *et al.* (2020). Germinating spores were observed with a stereo zoom microscope and transferred to potato dextrose agar (PDA; 39 g/L distilled water, Difco potato dextrose). The cultures were incubated at 25 °C for 4–6 wk, with weekly observations of growth and development.

DNA extraction, PCR amplification and sequencing

Mycelium was scraped from pure culture plates using a sterilized scalpel and used for DNA extraction using the BIOMIGA fungus genomic DNA extraction kit (Biomiga, San Diego, USA). For specimens without germinating ascospores, we extracted the DNA directly from the perithecial contents. All DNA samples were kept at -20 °C until analysed. Internal transcribed spacers (ITS), *TUB2 (ß-tubulin), and* RNA polymerase II second largest subunit *(rpb2*) were amplified by PCR with primers ITS1/ITS4 (White *et al*. 1990, Gardes & Bruns 1993), Bt2a/Bt2b or T1/T22 (Glass & Donaldson 1995, O'Donnell & Cigelnik 1997), and rpb2-5F/rpb2-7cR (Liu *et al.* 1999), respectively. The PCR mixture (25 µL) was composed as follows: 9.5 µL of double-distilled water, 12.5 µL of PCR Master Mix, 1 µL of each primer, and 1 µL of template DNA. The PCR amplification was conducted as reported by Samarakoon *et al*. (2022). Amplified products were checked through 1.5 % agarose gel electrophoresis stained with GoldenView, and were sent to Sangon Biotech Co., Ltd., China for sequencing.

Sequence alignments and phylogenetic analyses

All the assembled sequences were compared with each other and all the known sequences in GenBank using the BLAST algorithm for precise identification (https://www.ncbi.nlm.nih.gov) (Altschul *et al.* 1990). The molecular phylogeny was inferred from a combined dataset of ITS, *TUB2* and *rpb2* sequences. Reference sequences were retrieved from open databases originated from Kuhnert *et al.* (2017), and the Blastn results of close matches. Sequences were aligned using the MAFFT v. 7.110 online program (Katoh *et al.* 2019) with the default settings. The alignment was adjusted manually using BioEdit v. 7.0.5.3 (Hall 1999) where necessary. The maximum likelihood (ML) analysis was implemented in RAxML v. 8.2.12 using the GTRGAMMA substitution model with 1000 bootstrap replicates (Stamatakis 2014). The phylogenetic analyses were also performed for Bayesian inference in MrBayes v. 3.2.2 (Ronquist *et al*. 2012) online. The Markov chain Monte Carlo (MCMC) sampling in MrBayes v. 3.2.2 (Ronquist *et al*. 2012) was used to determine the posterior probabilities (PP). Six simultaneous Markov chains were run for 1 M generations, and trees were sampled every 1000 generation. The phylogenetic tree was visualized in FigTree v. 1.4.3 (Rambaut 2012). All analyses were run on the CIPRES Science Gateway v. 3.3 web portal (Miller *et al.* 2010). All the obtained sequences were deposited in GenBank (Table 1). The alignment file is attached to this paper as supplementary material (Data S1).

Chemotaxonomic studies

The stromal secondary metabolites were extracted and analysed using ultrahigh performance liquid chromatography coupled to diode array detection and ion mobility tandem mass spectrometry (UHPLC-DAD-IM-MS/MS) as previously described by Cedeño-Sanchez *et al*. (2023). Afterwards, the obtained features were dereplicated using our in-house database of authentic standards from secondary metabolites of hypoxylaceous taxa in MetaboScape 2022 (Bruker Daltonics, Bremen, Germany).

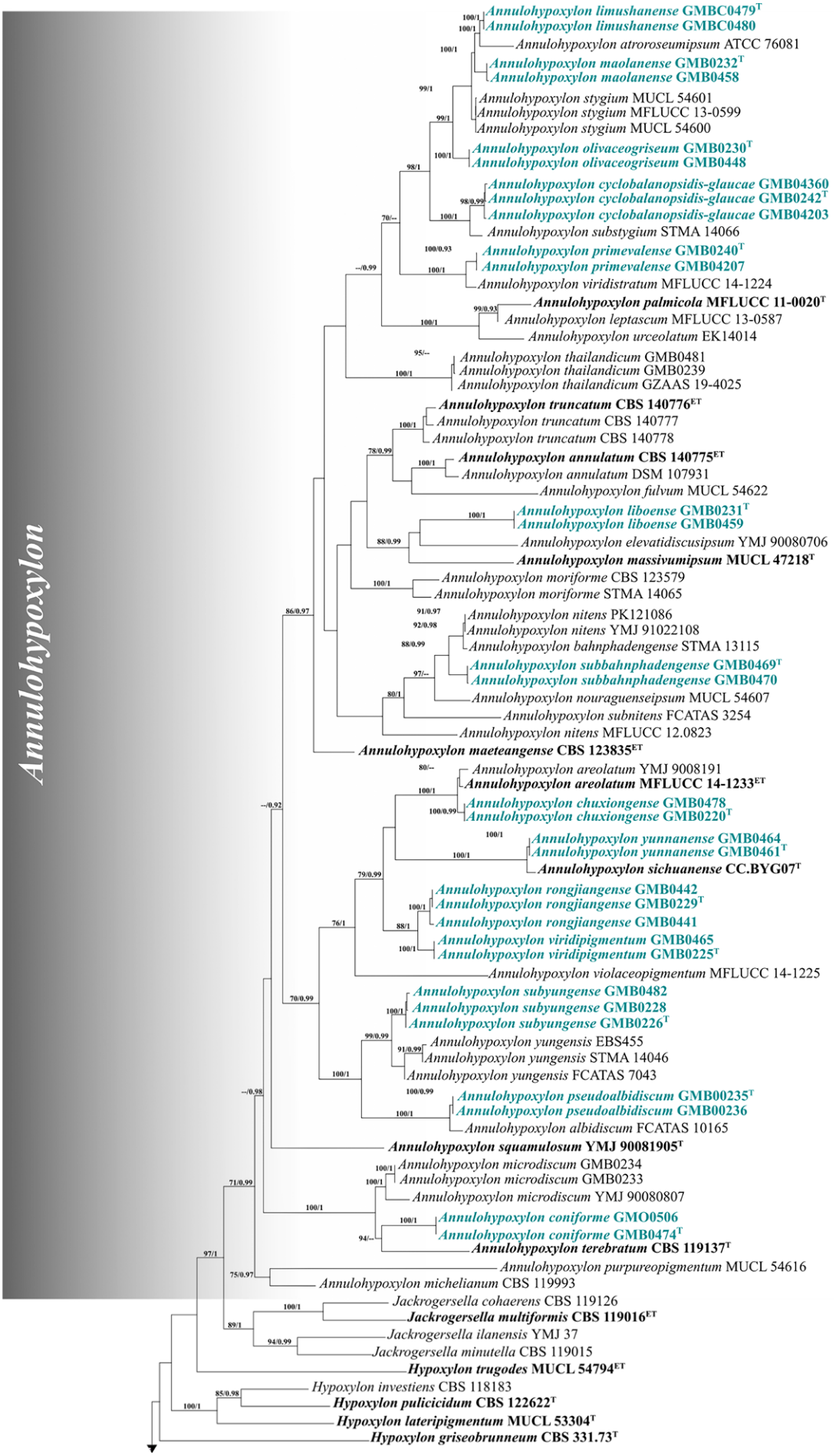

Fig. 2. RAxML tree based on a combined ITS, LSU, *rpb2* and *TUB2* sequences dataset. Bootstrap support values for maximum likelihood (ML) greater than 70 % and Bayesian posterior probabilities (BPP) greater than 0.90 are displayed above the respective branches (ML/BI). The newly described species are marked green. Type collections are in **bold**.

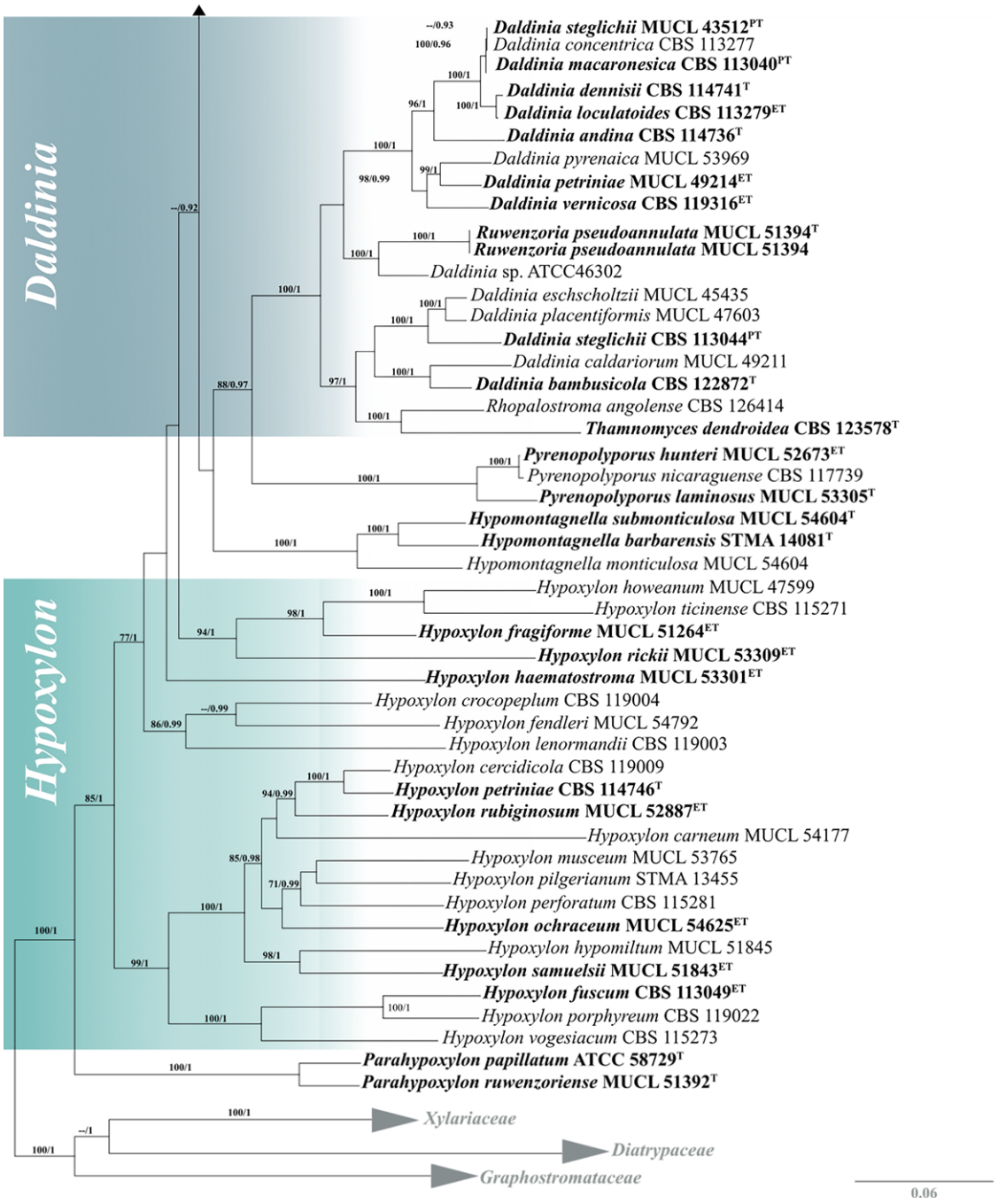

Fig. 2. (Continued)

RESULTS

Phylogeny

After the exclusion of ambiguously aligned regions and long gaps, the final combined data matrix contained 1450 characters. *Diatrype disciformis* (CBS 197.49), *Graphostroma platystomum* (CBS 270.87), *Xylaria arbuscula* (CBS 126415), and *X. hypoxylon* (CBS 122620) were added as outgroups. The tree topology derived from Maximum Likelihood (ML) analysis closely resembled that of Bayesian Inference (BI) analysis. The best-scoring RAxML tree is shown in Fig. 2.

The phylogenetic tree based on BI and ML approaches confirmed the position of our newly generated sequences nested within the phylogenetic clade of the genus *Annulohypoxylon* (Fig. 2). The results revealed fourteen new taxa at the species level, highlighted in red in the phylogram. Some nodes within the clades lacked robust support (they consistently appeared stable in repeated phylogenetic analyses), most other relationships obtained strong bootstrap support. According to the phylogenetic structure of the tree, *Annulohypoxylon* formed a large clade. However, the presence of *Rostrohypoxylon terebratum* (CBS 1119131) in the basal branch renders *Annulohypoxylon* status polyphyletic, as it forms well-supported sister clade with the new taxon *Annulohypoxylon coniforme* (GMB0474). The branch to which both species belong presented 94 % and 0.99 statistical values in the ML and BI analyses, respectively. This suggests that the taxonomic status of *Rostrohypoxylon terebratum* should be revisited for clarification (see note section *Annulohypoxylon terebratum*). The phylogenetic status of the isolated strains is discussed in the notes section of each taxon.

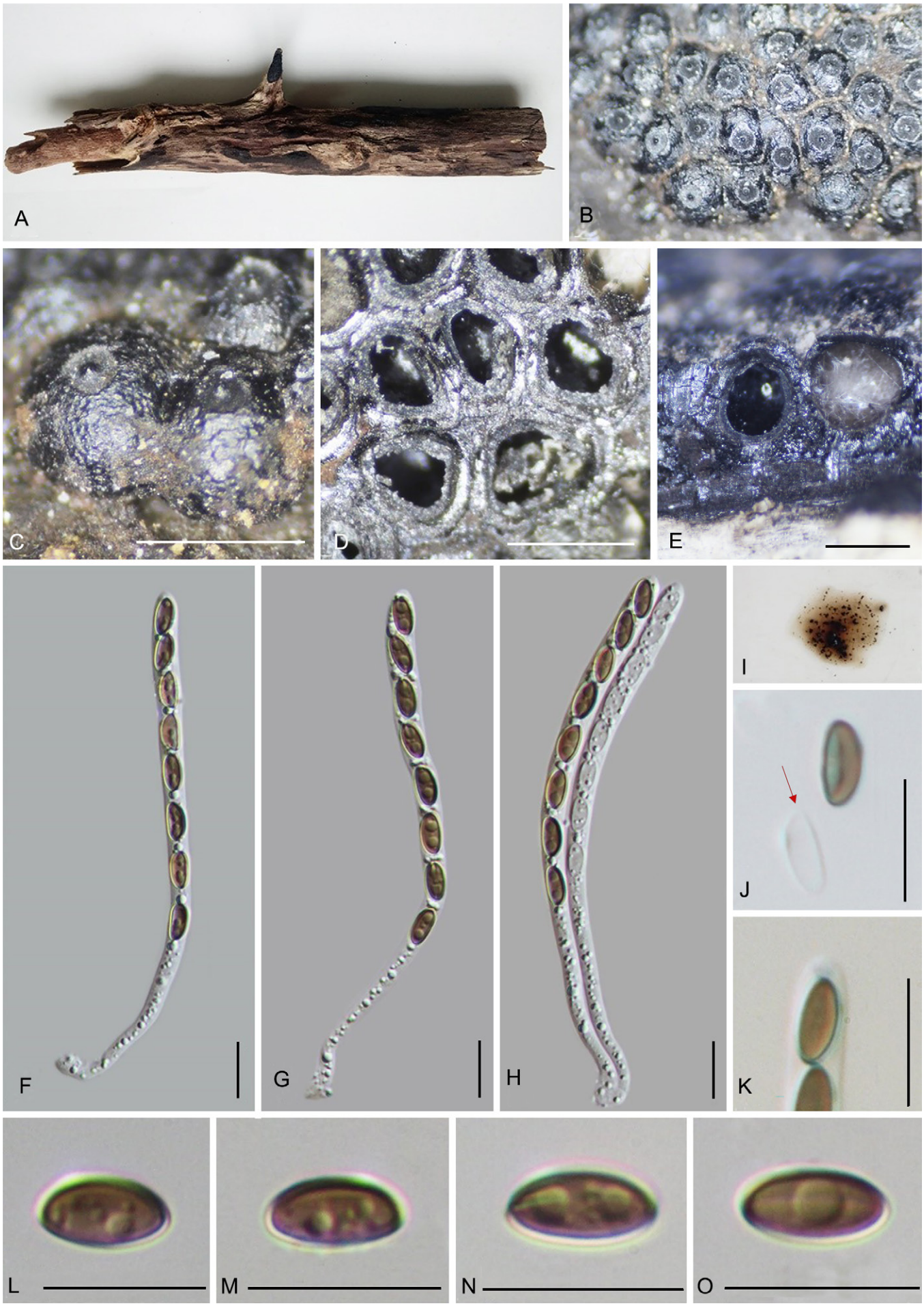

Fig. 3. *Annulohypoxylon bahnphadengense* (GMB0472). **A.** Stromatal habit on wood. **B.** Stromatal surface. **C.** Ostioles and ostiolar discs. **D.** Transverse section of stromata showing perithecia. **E.** Longitudinal section of the stromata showing perithecia. **F–H.** Asci in distilled water. **I.** Stromatal KOH-extractable pigment. **J.** Ascospores and perispore (arrow) dehiscent in 10 % KOH. **K.** Ascal apical apparatus (faintly blue in Melzer's reagent). **L–O.** Ascospores. Scale bars: D, E = 0.5 mm; F–H, J–O =10 µm.

Table 1. GenBank accession numbers used in this study. The newly generated sequences are marked **bold**. Type specimens are labeled with T (holotype), IT (isotype), PT (paratype) and ET (epitype).

Species	Strain number	Origin	GenBank Accession Number				References
			ITS	LSU	*rpb2*	*TUB2*	
Annulohypoxylon albidiscum	FCATAS 10165	China	—	PP359601	PP598934	—	Direct Submission
A. annulatum	DSM 107931	USA	MK287534	MK287546	MK287559	MK287572	Sir *et al.* (2015)
	CBS 140775	USA (ET)	KY610418	KY610418	KY624263	KX376353	Kuhnert *et al.* (2017; *TUB2*), Wendt *et al.* (2018: ITS, LSU, *rpb2*)
	YMJ 9008191	China	EF026141	—	—	AY951654	Hsieh *et al.* (2005)
A. areolatum	MFLUCC 14-1233	Thailand (ET)	KX376327	—	—	KX376344	Kuhnert *et al.* (2017)
A. atroroseum	ATCC 76081	Thailand	AJ390397	KY610422	KY624233	DQ840083	Kuhnert *et al.* (2014; ITS, *TUB2*), Wendt *et al.* (2018: LSU, *rpb2*)
A. bahnphadengense	STMA 13115	Thailand	KX376338	—	—	KX376347	Kuhnert *et al.* (2017)
A. coniforme	**GMB0474**	**China (T)**	**PQ278792**	**PQ278838**	**PQ273668**	**—**	**This study**
	GMB0506	**China**	**PQ278793**	**PQ278839**	**PQ273669**	**—**	**This study**
A. cyclobalanopsidis-glaucae	**GMB4360**	**China**	**PQ278768**	**PQ278812**	**PQ273642**	**PQ273677**	**This study**
	GMB0242	**China (T)**	**PQ278769**	**PQ278813**	**PQ273643**	**PQ273678**	**This study**
	GMB4203	**China**	**PQ278767**	**PQ278811**	**PQ273641**	**PQ273676**	**This study**
A. elevatidiscus	YMJ 90080706	China	—	—	—	AY951656	Hsieh *et al.* (2005)
A. fulvum	MUCL 54622	French Guiana	KX376337	—	—	KX376354	Kuhnert *et al.* (2017)
A. leptascum	MFLUCC 13-0587	Thailand	KU604576	—	—	KU604580	Sir *et al.* (2016)
A. maeteangense	CBS 123835	USA (ET)	OQ831977	OQ831977	—	—	Franco *et al.* (2022)
A. maolanense	**GMB0232**	**China (T)**	**PQ278764**	**PQ278808**	**PQ273638**	**PQ273673**	**This study**
	GMB0458	**China**	**PQ278763**	**PQ278807**	**PQ273637**	**PQ273672**	**This study**
A. massivum	MUCL 47218	Germany (T)	AM749938	—	—	KC977276	Bitzer *et al.* (2008)
A. michelianum	CBS 119993	Spain	KX376320	KY610423	KY624234	KX271239	Kuhnert *et al.* (2014; ITS, *TUB2*), Wendt *et al.* (2018; LSU, *rpb2*)
A. microdiscum	**GMB0234**	**China**	**PQ278791**	**PQ278837**	**PQ273667**	**PQ273702**	**This study**
	GMB0233	**China**	**PQ278790**	**PQ278836**	**PQ273666**	**PQ273701**	**This study**
A. microdiscus	YMJ 90080807	China	EF026137	—	—	AY951660	Hsieh *et al.* (2010)
A. moriforme	CBS 123579	Martinique	KX376321	KY610425	KY624289	KX271261	Kuhnert *et al.* (2016 ITS, *TUB2*), Wendt *et al.* (2018; LSU, *rpb2*)
	STMA 14065	Argentina	KU604561	—	—	KU159525	Sir *et al.* (2016)
A. nitens	PK121086	Thailand	KP134525	—	—	KP134518	Direct Submission
	YMJ 91022108	Thailand	AY951663	—	—	AY951663	Hsieh *et al.* (2005)

Table 1. (Continued).

Species	Strain number	Origin	GenBank Accession Number				References
			ITS	LSU	*rpb2*	*TUB2*	
	MFLUCC 12.0823	Thailand	KJ934991	KJ934992	KJ934994	KJ934993	Daranagama *et al.* (2015)
A. nouraguense	MUCL 54607	French Guiana	KX376335	—	—	KX376348	Kuhnert *et al.* (2017)
A. olivaceogriseum	**GMB0230**	**China (T)**	**PQ278766**	**PQ278810**	**PQ273640**	**PQ273675**	**This study**
	GMB0448	**China**	**PQ278765**	**PQ278809**	**PQ273639**	**PQ273674**	**This study**
A. palmicola	MFLUCC 11-0020	Thailand (T)	NG 068363	NG 071242	—	—	Ariyawansa *et al.* (2015)
A. primevalense	**GMB0240**	**China (T)**	—	**PQ278814**	**PQ273644**	**PQ273679**	**This study**
	GMB4207	**China**	—	**PQ278815**	**PQ273645**	**PQ273680**	**This study**
A. pseudoalbidiscum	**GMB0236**	**China**	**PQ278789**	**PQ278835**	**PQ273665**	**PQ273700**	**This study**
	GMB0235	**China (T)**	**PQ278788**	**PQ278834**	**PQ273664**	**PQ273699**	**This study**
A. purpureopigmentum	MUCL 54616	Germany	KC968942	—	—	KC977306	Kuhnert *et al.* (2014)
A. rongjiangense	**GMB0442**	**China**	**PQ278781**	**PQ278827**	**PQ273657**	**PQ273692**	**This study**
	GMB0229	**China (T)**	**PQ278780**	**PQ278826**	**PQ273656**	**PQ273691**	**This study**
	GMB0441	**China**	**PQ278782**	**PQ278828**	**PQ273658**	**PQ273693**	**This study**
A. sichuanense	CC.BYG07	China (T)	PP407890	PP407705	PP474173	**—**	Li & Guo (2019)
A. squamulosum	YMJ 90081905	China (T)	EF026139	—	—	AY951665	Hsieh *et al.* (2010)
A. stygium	MUCL 54601	French Guiana	KY610409	KY610475	KY624292	KX271263	Wendt *et al.* (2018)
	MFLUCC 13-0599	Thailand	KP401579	—	—	KP401586	Sir *et al.* (2015)
	MUCL 54600	French Guiana	KC968940	KY610474	KY624291	KC977304	Wendt *et al.* (2018)
A. subbahnphadengense	**GMB0469**	**China (T)**	**PQ278775**	**PQ278821**	**PQ273651**	**PQ273686**	**This study**
	GMB0470	**China**	**PQ278774**	**PQ278820**	**PQ273650**	**PQ273685**	**This study**
A. subnitens	FCATAS 3254	China	—	PP359599	PP598920	—	Direct Submission
A. substygium	STMA 14066	Argentina	KU604575	—	—	KU159526	Sir *et al.* (2016)
A. subyungense	**GMB0482**	**China**	**PQ278785**	**PQ278831**	**PQ273661**	**PQ273696**	**This study**
	GMB0226	**China (T)**	**PQ278787**	**PQ278833**	**PQ273663**	**PQ273698**	**This study**
	GMB0228	**China**	**PQ278786**	**PQ278832**	**PQ273662**	**PQ273697**	**This study**
A. thailandicum	**GMB0481**	**China**	**PQ278770**	**PQ278816**	**PQ273646**	**PQ273681**	**This study**
	GMB0239	**China**	**PQ278771**	**PQ278817**	**PQ273647**	**PQ273682**	**This study**
	GZAAS 19-4025	China	OR224993	OP612559	OR146904	—	Zhang *et al.* (2023)
A. truncatum	CBS 140777	USA	PP336482	PP336482	—	KU159524	Sir *et al.* (2016)
	CBS 140776	USA	KX376328	—	KY624276	KX376345	Kuhnert *et al.* (2014; ITS, *TUB2*), Wendt *et al.* (2018; *rpb2*)

Table 1. (Continued).

Species	Strain number	Origin	GenBank Accession Number				References
			ITS	LSU	*rpb2*	*TUB2*	
	CBS 140778	USA (ET)	KY610419	KY610419	KY624277	KX376352	Kuhnert *et al.* (2017; *TUB2*), Wendt *et al.* (2018; ITS, LSU, *rpb2*)
A. urceolatum	EK14014	Thailand	KP401582	—	—	KP401589	Sir *et al.* (2015)
A. violaceopigmentum	MFLUCC 14-1225	Thailand	KX376326	—	—	KX376343	Kuhnert *et al.* (2017)
A. viridipigmentum	**GMB0465**	**China**	**PQ278783**	**PQ278829**	**PQ273659**	**PQ273694**	**This study**
	GMB0225	**China (T)**	**PQ278784**	**PQ278830**	**PQ273660**	**PQ273695**	**This study**
A. viridistratum	MFLUCC 14-1224	Thailand	KX376325	—	—	KX376342	Kuhnert *et al.* (2017)
A. yungense	STMA 14046	Argentina	KX376323	—	—	KX376340	Kuhnert *et al.* (2017)
	EBS455	Argentina	KX376324	—	—	KX376341	Kuhnert *et al.* (2017)
	FCATAS 7043	China	—	PP356733	PP598922	PP598949	Direct Submission
A. limushanense	**GMB0479**	**China (T)**	**PQ278761**	**PQ278805**	**PQ273635**	**PQ273670**	**This study**
	GMB0480	**China**	**PQ278762**	**PQ278806**	**PQ273636**	**PQ273671**	**This study**
A. chuxiongense	**GMB0220**	**China (T)**	**PQ278776**	**PQ278822**	**PQ273652**	**PQ273687**	**This study**
	GMB0478	**China**	**PQ278777**	**PQ278823**	**PQ273653**	**PQ273688**	**This study**
A. liboense	**GMB0231**	**China (T)**	**PQ278773**	**PQ278819**	**PQ273649**	**PQ273684**	**This study**
	GMB0459	**China**	**PQ278772**	**PQ278818**	**PQ273648**	**PQ273683**	**This study**
A. yunnanense	**GMB0464**	**China**	**PQ278778**	**PQ278824**	**PQ273654**	**PQ273689**	**This study**
	GMB0462	**China (T)**	**PQ278779**	**PQ278825**	**PQ273655**	**PQ273690**	**This study**
Daldinia andina	CBS 114736	Ecuador (T)	AM749918	KY610430	KY624239	KC977259	Bitzer *et al.* (2008; ITS) as *D. grandis*, Kuhnert *et al.* (2014; *TUB2*), Wendth *et al.* (2018)
D. bambusicola	CBS 122872	Thailand (T)	KY610385	KY610431	KY624241	AY951688	Hsieh *et al.* (2005; *TUB2*), Wendt *et al.* (2018; ITS, LSU, *rpb2*)
D. caldariorum	MUCL 49211	France	AM749934	KY610433	KY624242	KC977282	Bitzer *et al.* (2008; ITS), Kuhnert *et al.* (2014; *TUB2*), Wendt *et al.* (2018; LSU, *rpb2*)
D. concentrica	CBS 113277	Germany	AY616683	KY610434	KY624243	KC977274	Triebel *et al.* (2005; ITS), Kuhnert *et al.* (2014; *TUB2*), Wendt *et al.* (2018; LSU, *rpb2*)
D. dennisii	CBS 114741	Australia (T)	JX658477	KY610435	KY624244	KC977262	Stadler *et al.* (2014; ITS), Kuhnert *et al.* (2014; *TUB2*), Wendt *et al.* (2018; LSU, *rpb2*)
D. eschscholtzii	MUCL 45435	Benin	JX658484	KY610437	KY624246	KC977266	Stadler *et al.* (2014; ITS), Kuhnert *et al.* (2014; *TUB2*), Wendt *et al.* (2018; LSU, *rpb2*)
D. loculatoides	CBS 113279	UK (ET)	AF176982	AF176982	AF176982	AF176982	Wendt *et al.* (2018)
D. macaronesica	CBS 113040	Spain (PT)	KY610398	KY610477	KY624294	KX271266	Wendt *et al.* (2018)
D. petriniae	MUCL 49214	Austria (ET)	AM749937	KY610439	KY624248	KC977261	Bitzer *et al.* (2008; ITS), Kuhnert *et al.* (2014; *TUB2*), Wendt *et al.* (2018; LSU, *rpb2*)

Table 1. (Continued).

Species	Strain number	Origin	GenBank Accession Number				References
			ITS	LSU	*rpb2*	*TUB2*	
D. placentiformis	MUCL 47603	Mexico	AM749921	KY610440	KY624249	KC977278	Stadler *et al.* (2014; ITS), Kuhnert *et al.* (2014; *TUB2*), Wendt *et al.* (2018; LSU, *rpb2*)
D. pyrenaica	MUCL 53969	France	KY610413	KY610413	KY624274	KY624312	Wendt *et al.* (2018)
D. sp.	ATCC 46302	USA	KY610389	KY610443	KY624253	KX271248	Wendt *et al.* (2018)
D. steglichii	MUCL 43512	Papua New Guinea (PT)	Y610399	KY610479	KY624250	KX271269	Wendt *et al.* (2018)
D. theissenii	CBS 113044	Argentina (PT)	KY610388	KY610441	KY624251	KX271247	Wendt *et al.* (2018)
D. vernicosa	CBS 119316	Germany (ET)	KY610395	KY610442	KY624252	KC977260	Kuhnert *et al.* (2014; *TUB2*), Wendt *et al.* (2018; ITS, LSU, *rpb2*)
Diatrype disciformis	CBS 197.49	Netherlands	—	DQ470964	DQ470915	—	Zhang *et al.* (2006)
Graphostroma platystomum	CBS 270.87	France (T)	JX658535	DQ836906	KY624296	HG934108	Stadler *et al.* (2014; ITS), Zhang *et al.* (2006; LSU), Koukol *et al.* (2015; *TUB2*), Wendt *et al.* (2018; *rpb2*)
Hypomontagnella barbarensis	STMA 14081	Argentina (T)	MK131720	MK131718	MK135891	MK135893	Lambert *et al.* (2019)
H. monticulosa	MUCL 54604	French Guiana	KY610404	KY610487	KY624305	KX271273	Wendt *et al.* (2018)
H. submonticulosa	CBS 115280	France	KC968923	KY610457	KY624226	KC977267	Kuhnert *et al.* (2014; ITS, *TUB2*), Wendt *et al.* (2018; LSU, *rpb2*)
Hypoxylon carneum	MUCL 54177	France	KY610400	KY610480	KY624297	KX271270	Wendt *et al.* (2018)
H. cercidicola	CBS 119009	France	KC968908	KY610444	KY624254	KC977263	Kuhnert *et al.* (2014; ITS, *TUB2*), Wendt *et al.* (2018; LSU, *rpb2*)
H. crocopeplum	CBS 119004	France	KC968907	KY610445	KY624255	KC977268	Kuhnert *et al.* (2014; ITS, *TUB2*), Wendt *et al.* (2018; LSU, *rpb2*)
H. fendleri	MUCL 54792	French Guiana	KF234421	KY610481	KY624298	KF300547	Kuhnert *et al.* (2014; ITS, *TUB2*), Wendt *et al.* (2018; LSU, *rpb2*)
H. fragiforme	MUCL 51264	Germany (ET)	KC477229	KM186295	MK887342	KX271282	Stadler *et al.* (2013; ITS), Daranagama *et al.* (2015; LSU, *rpb2*), Wendt *et al.* (2018; *TUB2*)
H. fuscum	CBS 113049	Germany (ET)	KY610401	KY610482	KY624299	KX271271	Wendt *et al.* (2018)
H. griseobrunneum	CBS 331.73	India (T)	KY610402	KY610483	KY624300	KC977303	Kuhnert *et al.* (2014; *TUB2*), Wendt *et al.* (2018; ITS, LSU, *rpb2*)
H. haematostroma	MUCL 53301	Martinique (ET)	KC968911	KY610484	KY624301	KC977291	Kuhnert *et al.* (2014; ITS, *TUB2*), Wendt *et al.* (2018; LSU, *rpb2*),
H. howeanum	MUCL 47599	Germany	AM749928	KY610448	KY624258	KC977277	Bitzer *et al.* (2008; ITS), Kuhnert *et al.* (2014; *TUB2*), Wendt *et al.* (2018; LSU, *rpb2*)
H. hypomiltum	MUCL 51845	Guadeloupe	KY610403	KY610449	KY624302	KX271249	Wendt *et al.* (2018)
H. investiens	CBS 118183	Malaysia	KC968925	KY610450	KY624259	KC977270	Kuhnert *et al.* (2014; ITS, *TUB2*), Wendt *et al.* (2018; LSU, *rpb2*)

Table 1. (Continued).

Species	Strain number	Origin	GenBank Accession Number				References
			ITS	LSU	*rpb2*	*TUB2*	
H. lateripigmentum	MUCL 53304	Martinique (T)	KC968933	KY610486	KY624304	KC977290	Kuhnert *et al.* (2014; ITS, *TUB2*), Wendt *et al.* (2018; LSU, *rpb2*)
H. lenormandii	CBS 119003	Ecuador	KC968943	KY610452	KY624261	KC977273	Kuhnert *et al.* (2014; ITS, *TUB2*), Wendt *et al.* (2018; LSU, *rpb2*)
H. musceum	MUCL 53765	Guadeloupe	KC968926	KY610488	KY624306	KC977280	Kuhnert *et al.* (2014; ITS, *TUB2*), Wendt *et al.* (2018; LSU, *rpb2*)
H. ochraceum	MUCL 54625	Martinique (ET)	KC968937	—	KY624271	KC977300	Kuhnert *et al.* (2014; ITS, *TUB2*), Wendt *et al.* (2018; *rpb2*)
H. perforatum	CBS 115281	France	KY610391	KY610455	KY624224	KX271250	Wendt *et al.* (2018)
H. petriniae	CBS 114746	France (T)	KY610405	KY610491	KY624279	KX271274	Wendt *et al.* (2018)
H. pilgerianum	STMA 13455	Martinique	KY610412	KY610412	KY624308	KY624315	Wendt *et al.* (2018)
H. porphyreum	CBS 119022	France	KC968921	KY610456	KY624225	KC977264	Kuhnert *et al.* (2014; ITS, *TUB2*), Wendt *et al.* (2018; LSU, *rpb2*)
H. pulicicidum	CBS 122622	Martinique (T)	JX183075	KY610492	KY624280	JX183072	Bills *et al.* (2012; ITS, *TUB2*), Wendt *et al.* (2018; LSU, *rpb2*)
H. rickii	MUCL 53309	Martinique (ET)	KC968932	KY610416	KY624281	KC977288	Kuhnert *et al.* (2014; ITS, *TUB2*), Wendt *et al.* (2018; LSU, *rpb2*)
H. rubiginosum	MUCL 52887	Germany (ET)	KC477232	KY610469	KY624266	KY624311	Stadler *et al.* (2013; ITS), Wendt *et al.* (2018; *TUB2*, LSU, *rpb2*)
H. samuelsii	MUCL 51843	Guadeloupe (ET)	KC968916	KY610466	KY624269	KC977286	Kuhnert *et al.* (2014; ITS, *TUB2*), Wendt *et al.* (2018; LSU, *rpb2*)
H. ticinense	CBS 115271	France	JQ009317	KY610471	KY624272	AY951757	Hsieh *et al.* (2005; ITS, *TUB2*), Wendt *et al.* (2018; LSU, *rpb2*)
H. trugodes	MUCL 54794	Sri Lanka (ET)	KF234422	KY610493	KY624282	KF300548	Kuhnert *et al.* (2014; ITS, *TUB2*), Wendt *et al.* (2018; LSU, *rpb2*)
H. vogesiacum	CBS 115273	France	KC968920	KY610417	KY624283	KX271275	Kuhnert *et al.* (2014; ITS), Kuhnert *et al.* (2017; *TUB2*), Wendt *et al.* (2018; LSU, *rpb2*)
Jackrogersella cohaerens	CBS 119126	Germany	KY610396	KY610497	KY624270	KY624314	Wendt *et al.* (2018)
J. ilanensis	YMJ 37	China	—	—	—	AY951657	Hsieh *et al.* (2005)
J. minutella	CBS 119015	Portugal	KY610381	KY610424	KY624235	KX271240	Kuhnert *et al.* (2017; *TUB2*), Wendt *et al.* (2018: ITS, LSU, *rpb2*)
J. multiformis	CBS 119016	Germany (ET)	KC477234	KY610473	KY624290	KX271262	Kuhnert *et al.* (2014; ITS), Kuhnert *et al.* (2017; *TUB2*), Wendt *et al.* (2018; LSU, *rpb2*)
Parahypoxylon papillatum	ATCC 58729	USA (T)	KC968919	KY610454	KY624223	KC977258	Kuhnert *et al.* (2014; ITS, *TUB2*), Wendt *et al.* (2018; LSU, *rpb2*)
P. ruwenzoriense	MUCL 51392	D. R. Congo (T)	ON792786	ON954156	OP251039	ON813078	Cedeño-Sanchez *et al.* (2023)
P. hunteri	MUCL 52673	Ivory Coast (ET)	KY610421	KY610472	KY624309	KU159530	Kuhnert *et al.* (2017; *TUB2*), Wendt *et al.* (2018; ITS, LSU, *rpb2*)

Table 1. (Continued).

Species	Strain number	Origin	GenBank Accession Number				References
			ITS	LSU	*rpb2*	*TUB2*	
P. laminosus	MUCL 53305	Martinique (T)	KC968934	KY610485	KY624303	KC977292	Kuhnert *et al.* (2014; ITS, *TUB2*), Wendt *et al.* (2018; LSU, *rpb2*)
P. nicaraguense	CBS 117739	Burkina Faso	AM749922	KY610489	KY624307	KC977272	Bitzer *et al.* (2008; ITS), Kuhnert *et al.* (2014; *TUB2*), Wendt *et al.* (2018; LSU, *rpb2*)
Rhopalostroma angolense	CBS 126414	Ivory Coast	KY610420	KY610459	KY624228	KX271277	Wendt *et al.* (2018)
Rostrohypoxylon terebratum	CBS 119137	Thailand (T)	DQ631943	DQ840069	DQ631954	DQ840097	Tang *et al.* (2009), Fournier *et al.* (2010)
Ruwenzoria pseudoannulata	MUCL 51394	D. R. Congo (T)	KY610406	KY610494	KY624286	KX271278	Wendt *et al.* (2018)
Thamnomyces dendroidea	CBS 123578	French Guiana (T)	FN428831	KY610467	KY624232	KY624313	Stadler *et al.* (2010; ITS), Wendt *et al.* (2018; *TUB2*, LSU, *rpb2*)
Xylaria arbuscula	CBS 126415	Germany	KY610394	KY610463	KY624287	KX271257	Fournier *et al.* (2011; ITS), Wendt *et al.* (2018; *TUB2*, LSU, *rpb2*)
X. hypoxylon	CBS 122620	Sweden (ET)	KY610407	KY610495	KY624231	KX271279	Wendt *et al.* (2018)

TAXONOMY

Annulohypoxylon bahnphadengense J. Fourn. & M. Stadler, *Fungal Diversity* **40**: 30. 2010. MB 512545. Fig. 3.

Sexual morph: *Stromata* on the surface of dead wood effused-pulvinate, surface Dark Vinaceous (114) to Black, hard-textured, 1/4 exposed perithecial mounds, carbonaceous, 0.5–6 cm long, 0.8–3 cm wide, 0.9–1.5 mm high ($\bar{x}$ = 4.2 cm × 1.8 cm × 1 mm, *n* = 10), tissue between and below the perithecia black; with 10 % KOH extractable pigments greyish sepia (106). *Perithecia* spherical, 354–463 µm diam. ($\bar{x}$ = 404.5 µm, *n* = 20), ostioles conical papillate, encircled with a truncatum-type disc, 0.2–0.3 mm diam. *Asci* 105–153 × 4–5 µm ($\bar{x}$ = 128.8 × 4.5 µm, *n* = 30), 8-spored, unitunicate, cylindrical, long-stipitate, the stipes 37–75 µm long ($\bar{x}$ = 62.5 µm, *n* = 30), the spore-bearing parts 45–78 µm long ($\bar{x}$ = 66.2 µm, *n* = 30), with apical apparatus faintly bluing in Melzer's reagent, discoid, inconspicuous. *Ascospores* 6–10.5 × 3–4.5 µm ($\bar{x}$ = 8.7 × 4 µm, *n* = 30), uniseriate, unicellular, inequilateral ellipsoid, with rounded ends, brown, with straight germ slit covering the full spore length on the convex side, perispore dehiscent in 10 % KOH, smooth with a thickening on the convex side, epispore smooth. *Asexual morph* not observed.

Secondary metabolites: Stromata contain several unknown metabolites, as well as truncatone A and hinnulin A according to the MS/MS analysis.

Material examined: **China**, Hainan Province, Wenchang City, Tongguling 19°39'38.13"N, 111°0'50.55"E, tropical forest, on dead wood of an unknown plant, 8 Nov. 2020, *Y.H. Pi*, 2020TGL3 (GMB0472, culture GMBC0472).

Notes: The morphological characters of our collection are congruent with *A. bahnphadengense* except for slightly larger ascospores. Additionally, the ITS (PV076878) sequence BLAST result confirmed the similarity of our collection to *A. bahnphadengense*. Morphologically, *A. bahnphadengense* is similar to *A. nitens*, but *A. nitens* differs in having a bovei-type ostiolar disc and yielding greenish olivaceous (90) pigments in KOH. *Annulohypoxylon bahnphadengense* has previously been documented in Thailand (Fournier & Lechat 2016, Kuhnert *et al.* 2017). This study marks its first recorded presence in China.

Annulohypoxylon chuxiongense H.M. Hu, K. Habib & Q.R. Li, ***sp. nov.*** MB 855586. Fig. 4.

Etymology: Refers to the locality of the type specimen, Chuxiong City.

Sexual morph: *Stromata* on the surface of dead wood effused-pulvinate, hemispherical, slightly constricted at base, with perithecial mounds up to 1/3 exposed, tissue below the perithecial layer black, 5–30 mm long, 5–10 mm wide, 0.5–0.8 mm high ($\bar{x}$ = 20 × 6 × 0.7 mm, *n* = 10), surface black, carbonaceous; with 10 % KOH extractable pigments grey olivaceous (107) to dull green (70). *Perithecia* 475–630 µm wide, 457–645 µm high ($\bar{x}$ = 518 × 535 µm, *n* = 20), spherical, ostioles conical papillate, encircled with a bovei-type disc, 0.35–0.45 mm diam. *Asci* 120–135 µm ($\bar{x}$ = 125,

n = 30), 8-spored, unitunicate, cylindrical, long-stipitate the stipes 45–65 µm long, ($\bar{x}$ = 55.2 µm, *n* = 30), the spore-bearing parts 70–75 µm long, 5–5.7 µm wide, ($\bar{x}$ = 73 × 5.5 µm, *n* = 30), apical apparatus not bluing in Melzer's reagent, inconspicuous. *Ascospores* 8–9 × 3.5–5 µm ($\bar{x}$ = 8.5 × 4.5 µm, *n* = 30), uniseriate, unicellular, inequilateral ellipsoid, brown, with rounded ends, with conspicuous straight germ slit covering the full spore length on the convex side, perispore dehiscent in 10 % KOH, smooth with a thickening on the convex side, epispore smooth.

Asexual morph on OA: *Conidiophores* periconiella-like, as defined in Ju & Rogers (1996), yellow to brown, roughened. *Conidiogenous cells* yellow, smooth, 9.5–11.5 × 3.4–5.5 µm ($\bar{x}$ = 10.6 × 4.7 µm, n = 30). *Conidia* hyaline, smooth, ellipsoid, 2.5–3.5 µm × 2.9–4.5 µm ($\bar{x}$ = 3.1 × 3.9 µm, n = 30).

Culture characteristics: Colonies growing on OA at 25 °C for 3 wk, with a diameter of 5 cm. Surface colonies are lavender grey (125), felty, cottony, flocculent, azonate, with diffuse margins, with scattered black patches; reverse dark mouse grey (119) to olivaceous grey (121).

Secondary metabolites: Stromata contain truncatone A and C according to the MS/MS analysis.

Typus: **China**, Yunnan Province, Chiang Dao, Chuxiong City, Great Montenegro 23°37'50.24"N, 100°3'33.48"E, subtropical forest, on dead branches, 11 Sep. 2021, *Y.H. Pi*, 2021DHS8 (**holotype** GMB0220, ex-type culture GMBC0220; **isotype** KUN-HKAS 129498).

Barcodes: ITS = PQ278776, LSU = PQ278822, *rpb2* = PQ273652, *TUB2* = PQ273687.

Additional material examined: **China**, Yunnan Province, Chuxiong City, Zixi Mountain Forest Park, 25°1'15.13"N, 107°23'48.44"E, on dead wood, 8 Aug. 2021, *Y.H. Pi*, 2021ZXS3 (**paratype** GMB0478, culture GMBC0478).

Notes: Morphologically and phylogenetically, *A. chuxiongense* is closely related to *A. areolatum*, as both share the same ascospore morphology and yield green stromatal KOH-extractable pigment. However, the latter has a surface colour ranging from sepia (116) to grey olivaceous (107) (vs blackish), larger perithecia 0.5–1 mm diam. (vs 0.35–0.45 mm), and a larger ostiolar disc 0.3–0.7 mm diam. (vs 0.35–0.45 mm). Additionally, the stromata of *A. areolatum* usually contain only up to 10 perithecia (vs more than 10) and have longer asci (121–181 µm) with a longer stipe of 45–110 µm (Kuhnert *et al.* 2017).

Morphologically, *A. chuxiongense* is similar to *A. bovei* except that the latter has larger ascospores (10.5–13 × 5–6.5 µm) with a germ slit shorter than the spore length, and lacks KOH-extractable pigments in mature stromata (Kuhnert *et al*. 2017).

Annulohypoxylon coniforme H.M. Hu, K. Habib & Q.R. Li, ***sp. nov.*** MB 855587. Fig. 5.

Etymology: Refers to the conical ostiole of the perithecia.

Sexual morph: *Stromata* on the surface of dead wood, pulvinate, with inconspicuous perithecial mounds, surface black, 0.4–1.2 cm long, 0.2–0.4 cm broad, 0.4–0.9 mm thick, carbonaceous, tissue black between perithecia, with 10 % KOH extractable pigments pale purplish grey (127). *Perithecia* 150–300 µm high, 150– 200 µm wide, obovoid to spherical, with a top of tapered, conical structure, ostioles opening at the broadly rounded top of tapered structure, conical necks 0.2–0.35 mm diam. at the base. *Asci* 93–110 × 4–6.5 µm ($\bar{x}$ = 100 × 5.2 µm, *n* = 30), 8-spored, unitunicate, cylindrical, long-stipitate, the stipes 36–54 µm long ($\bar{x}$ = 42 µm, *n* = 30), the spore-bearing parts 47–59 µm long ($\bar{x}$ = 52 µm, *n* = 30), with apparent apical apparatus, bluing in Melzer's reagent, 0.8–1 µm wide, 1.5–1.8 µm high. *Ascospores* 6.5–7.8 × 3–4 µm ($\bar{x}$ = 7.3 × 3.3 µm, *n* = 60), uniseriate, unicellular, inequilateral ellipsoidal with narrowly rounded ends, with a faint straight germ slit 4/5 to almost spore length on the convex side, perispore dehiscent in 10 % KOH, smooth with a thickening on the convex side, epispore smooth.

Asexual morph on OA: *Conidiophores* sporothrix-like to virgariella-like, hyaline, smooth to finely roughened. *Conidiogenous cells* hyaline, smooth to finely roughened, 32.5–45 × 2–2.5 µm ($\bar{x}$ = 38.8 × 2.2 µm, *n* = 15). *Conidia* hyaline, smooth, ovoid, 3–4 × 1.9–2.9 µm ($\bar{x}$ = 3.6 × 2.5 µm, *n* = 30).

Culture characteristics: Colonies on OA reaching the edge of the Petri dish 5 cm in 3 wk, zonate, white, felty, cottony, thin; reverse smoke grey (105).

Secondary metabolites: Stromata did not contain prominent secondary metabolites, yet presented fatty acid-like molecules and other yet unknown metabolites according to the MS/MS analysis.

Typus: **China**, Hainan Province, Qiongzhong County, Limushan Nature Reserve, 19°12'28.95"N, 109°50'21.74"E, subtropical forest, on dead wood, 12 Nov. 2020, *Y.H. Pi*, 2020QZ90 (**holotype** GMB0474, ex-type culture GMBC0474; **isotype** KUN-HKAS 129504).

Barcodes: ITS = PQ278792, LSU = PQ278838, *rpb2* = PQ273668.

Additional materials examined: **China**, Yunnan Province, Chuxiong City, Zixi Mountain Forest Park, 25°1'15.13"N, 107°23'48.44"E, tropical forest, on dead wood, 8 Aug. 2021, *Y.H. Pi*, ZX2021_21 (**paratype** GMB0506, culture GMBC0506).

Notes: Phylogenetically and morphologically, *Annulohypoxylon coniforme* is closely related to *A. terebratum* (previously known as *Rostrohypoxylon terebratum*), sharing protruding ostiolar neck perithecia (Fournier *et al.* 2010). However, *A. terebratum* is characterized by its erumpent effused stromata featuring stout, strongly protruding ostiolar necks, asci without an apparent apical apparatus and ascospores are cylindrical with broadly rounded ends which distinguishes it from *Annulohypoxylon coniforme*. Moreover, *A. terebratum* has large perithecia 0.6–1 mm in height and 0.5–0.6 mm diam., with large ostiolar necks 0.25–0.5 mm

Fig. 4. *Annulohypoxylon chuxiongense* (GMB0220, holotype). **A.** Stromatal habit on wood. **B.** Stromatal surface. **C.** Ostioles and ostiolar discs. **D.** Transverse section of stromata showing perithecia. **E.** Longitudinal section of the stromata showing perithecia. **F.** Ascus in distilled water. **G.** Stromatal KOH-extractable pigment. **H.** Perispore dehiscent in 10 % KOH. **I.** Ascal apical apparatus (non-bluing in Melzer's reagent). **J, K.** Periconiella-like conidiophores. **L, M.** Conidia. **N, O.** Ascospores. **P, Q.** Colonies on OA (P-upper, Q-lower). Scale bars: C–E = 0.5 mm; F–M = 10 µm; N–O = 5 µm.

Fig. 5. *Annulohypoxylon coniforme* (GMB0474, holotype). **A.** Stromatal habit on wood. **B.** Stromatal surface with ostioles. **C.** Ostioles. **D.** Longitudinal section of the stromata showing perithecia. **E.** Transverse section of stromata. **F, G.** Asci in distilled water. **H.** Sporothrix-like to Virgariella-like conidiophore. **I.** Conidia. **J.** Stromatal KOH-extractable pigment. **K.** Perispore dehiscent in 10 % KOH. **L.** Ascal apical apparatus (stained in Melzer's reagent). **M–P.** Ascospores. Scale bars: D, E = 0.5 mm; F–I; K–P = 10 µm.

in height. The chemistry also differs, *A. terebratum* yields a greenish olivaceous pigment in KOH, whereas *A. coniforme* yields a mouse grey (119) olivaceous grey (121) pigment (Fournier *et al.* 2010). However, it should be noted that the pigmentation could not be associated to previously reported pigments in the *Hypoxylaceae*.

In the phylogram (Fig. 2), *A. coniforme*, *A. microdiscum*, and *A. terebratum* form a well-supported clade. No protruding ostiolar neck perithecia without a disc are described in *A. microdiscum* (Kuhnert *et al.* 2017).

Annulohypoxylon cyclobalanopsidis-glaucae Y.H. Pi, K. Habib & Q.R. Li, ***sp. nov.*** MB 855588. Fig. 6.

Etymology: Refers to the host, *Cyclobalanopsis glauca.*

Sexual morph: *Stromata* on the surface of dead wood effused-pulvinate, surface Brown Vinaceous (84), with perithecial mounds 1/4 exposed, carbonaceous, 1.3–2 cm long, 0.2–0.7 cm wide, 0.6–0.7 mm high ($\bar{x}$ = 1.5 cm × 0.5 cm × 0.5 mm, *n* = 8), tissue below the perithecial layer black, with 10 % KOH extractable pigments dark mouse grey (119). *Perithecia* 324–364 µm wide, 355–391 µm high ($\bar{x}$ = 341 × 376 µm, *n* = 20), spherical to obovoid; ostioles papillate, encircled with a bovei-type disc, 0.15–0.21 mm diam. *Asci* 80–105 × 4.5–6 µm ($\bar{x}$ = 92 × 5 µm, *n* = 30), 8-spored, unitunicate, cylindrical, long-stipitate, the stipes 30–45 µm long ($\bar{x}$ = 35 µm, *n* = 30), the spore-bearing parts 65–78 µm long ($\bar{x}$ = 68 µm, *n* = 30), apical apparatus not bluing in Melzer's reagent, discoid, inconspicuous. *Ascospores* 6–7 × 3–4 µm ($\bar{x}$ = 6.5 × 3.5 µm, *n* = 30), uniseriate, unicellular, inequilateral ellipsoid, with rounded ends, brown, with straight germ slit covering the full spore length on the flattened side, perispore dehiscent in 10 % KOH, smooth with a thickening on the flattened side, epispore smooth. *Asexual morph* not observed.

Culture characteristics: Colonies on OA reaching the edge of the Petri dish 5 cm in 3 wk, azonate, white, felty, cottony, with scattered black patches in the middle; reverse luteous (12) to ochreous (44) with white edges. Not sporulating on OA nor on PDA.

Secondary metabolites: Stromata contain hypoxylonol C/F and related molecules as major metabolites according to the MS/MS analysis.

Typus: **China**, Yunnan Province, Baoshan City, Wayao Town, 25°32'14.15"N, 99°28'50.98"E, subtropical forest, on dead wood of *Cyclobalanopsis glauca*, 3 Aug. 2021, *Y.H. Pi*, 2021WYZ8 (**holotype** GMB0242, ex-type culture GMBC0242; **isotype** KUN-HKAS 129505).

Barcodes: ITS = PQ278769, LSU = PQ278813, *rpb2* = PQ273643, *TUB2* = PQ273678.

Additional materials examined: **China**, Guangxi Zhuang Autonomous Region, Daming Mountain National Nature Reserve, 22°22′15.84″N, 107°11′16.97″E, on dead wood, 4 Aug. 2023, *H.M. Hu*, 2023DMS6 (**paratype** GMB4203); Yunnan Province, Dawei Mountain National Nature Reserve 27°57' 30.59"N, 103°52' 36.89"E, on dead wood, 18 Jul. 2023, *H.M. Hu*, 2023DWS15, GMB4360.

Notes: In the phylogram (Fig. 2), *Annulohypoxylon cyclobalanopsidis-glaucae* is closely related to *A. substygium*. Morphologically, both also share many similarities, such as similar stromatal colouration and ascospore size, with a germ slit on the flattened side of ascospores. However, the latter has stromata with inconspicuous perithecial mounds up to 1/2 exposed, larger perithecia 0.4–0.6 mm in height and 0.3–0.5 mm in width, with a large disc 0.25–0.35 mm diam., and immature stromata yield fuscous black (70) whereas mature give fawn (87) pigments in KOH. Moreover, the ascospores of *A. substygium* are ellipsoid and nearly equilateral, with broadly rounded ends (Kuhnert *et al*. 2017, Sir *et al*. 2018). Morphologically, it is also close to *A. stygium* which has also smaller ostiolar discs of truncatum-type and a similar ascospore size. However, *A. stygium* has larger perithecia (0.3–0.5 × 0.2–0.3 mm) and yields greenish olivaceous (90) to dull green (70) pigments in KOH (Fournier & Lechat 2016).

Annulohypoxylon liboense Y.H. Pi, K. Habib & Q.R. Li, ***sp. nov.*** MB 855589. Fig. 7.

Etymology: Refers to the collection location, Libo city.

Sexual morph: *Stromata* on the surface of the dead branch effused-applanate, not smooth, with inconspicuous perithecial mounds up to less than 1/4 exposed; surface black, carbonaceous, 1–3.5 cm long, 0.7–1.5 cm wide, 0.8–1 mm high, tissue below the perithecial layer brown to black; with 10 % KOH extractable pigments dull green (70). *Perithecia* 270–368 µm wide, 200–431 µm high ($\bar{x}$ = 340 × 341 µm, *n* = 20), spherical, ostioles conical papillate, encircled with a truncatum-type disc, 0.35–0.5 mm diam. *Asci* 130–155 × 5–7 µm ($\bar{x}$ = 138 × 6 µm, *n* = 30), 8-spored, unitunicate, cylindrical, long-stipitate, the stipes 60–95 µm long ($\bar{x}$ = 80 µm, *n* = 30), the spore-bearing parts 70–80 µm long ($\bar{x}$ = 72 µm, *n* = 30), with apical apparatus bluing in Melzer's reagent, discoid, 1.5–2 × 0.6–0.9 µm ($\bar{x}$ = 1.8 × 0.7 µm, *n* = 20). *Ascospores* 8–10 × 3–4.7 µm ($\bar{x}$ = 8.5 × 3.5 µm, *n* = 30), uniseriate, unicellular, inequilateral ellipsoid with narrowly rounded ends, brown, with a faint straight germ slit nearly the spore length on the convex side, perispore dehiscent in 10 % KOH, smooth with a thickening on the convex side, epispore smooth.

Asexual morph on OA: *Conidiophores* sporothrix-like to virgariella-like, hyaline, smooth to finely roughened. *Conidiogenous cells* hyaline, smooth to finely roughened, 20–36 × 2.5–3.5 µm ($\bar{x}$ = 29 × 3 µm, *n* = 20). *Conidia* hyaline, smooth to finely roughened, ovoid, 2–2.6 × 3.4–4.8 µm ($\bar{x}$ = 2.4 × 4.1 µm, *n* = 30).

Culture characteristics: Colonies on OA reaching the edge of the Petri dish 5 cm in 3 wk, azonate, surface white, velvety to felty, irregular entire margin; reverse dull green (70).

Secondary metabolites: Stromata contain several yet unknown azaphilone-like compounds and other fatty acid-like molecules according to the MS/MS analysis.

Typus: **China**, Guizhou Province, Libo County, Qiannan Buyi and Miao Autonomous Prefecture, Maolan National Nature Reserve, 25°18'2.73"N, 108°4'29.49"E, subtropical moist broadleaf forest, on dead branch, 9 Jul. 2021, *Y.H.*

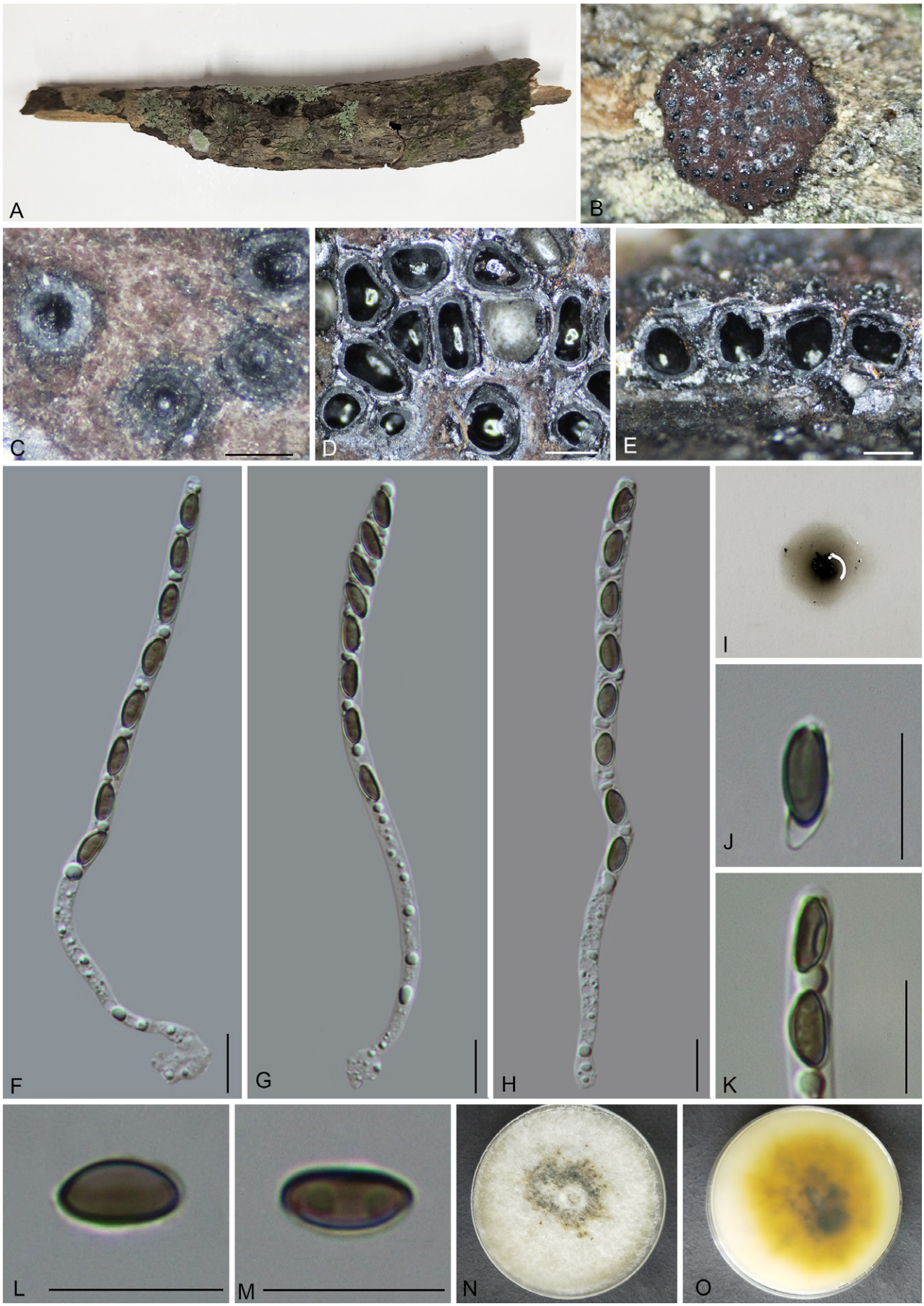

Fig. 6. *Annulohypoxylon cyclobalanopsidis-glaucae* (GMB0242, holotype). **A.** Stromatal habit on wood. **B.** Stromatal surface. **C.** Ostioles and ostiolar discs. **D.** Transverse section of stromata. **E.** Longitudinal section of the stromata showing perithecia. **F–H.** Asci in distilled water. **I.** Stromatal KOH-extractable pigment. **J.** Perispore dehiscent in 10 % KOH. **K.** Ascal apical apparatus (non-bluing in Melzer's reagent). **L, M.** Ascospores. **N, O.** Colonies on OA (N-upper, O-lower). Scale bars: D, E = 0.5 mm; F–H, J–M = 10 µm.

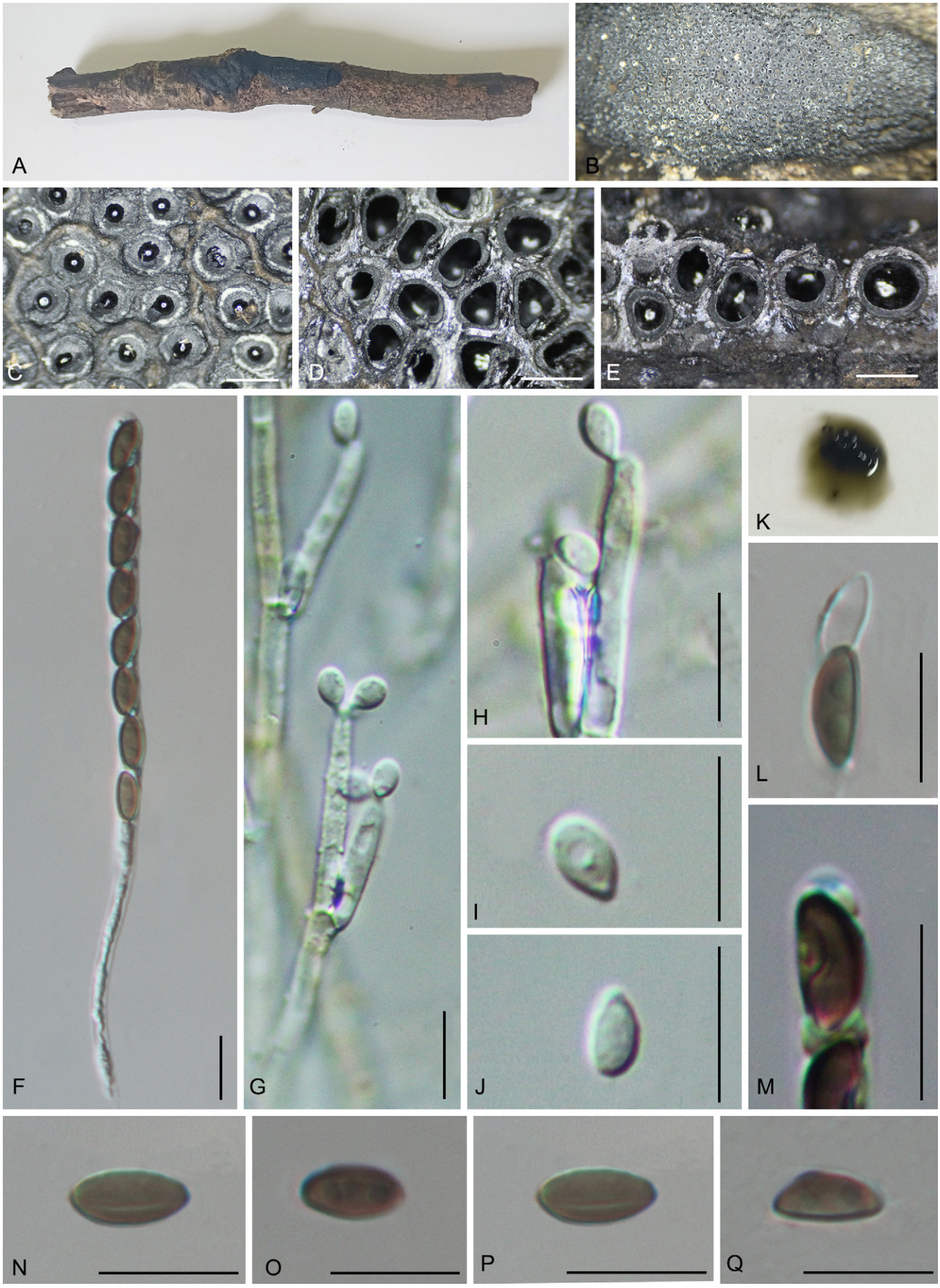

Fig. 7. *Annulohypoxylon liboense* (GMB0231, holotype). **A.** Stromatal habit on wood. **B.** Stromatal surface. **C.** Ostioles and ostiolar discs. **D.** Transverse section of stromata showing perithecia. **E.** Longitudinal section of the stromata showing perithecia. **F.** Ascus in distilled water. **G, H.** Sporothrix-like to Virgariella-like conidiophore. **I, J.** Conidia. **K.** Stromatal KOH-extractable pigment. **L.** Perispore dehiscent in 10 % KOH. **M.** Ascal apical apparatus (stained in Melzer's reagent). **N–Q.** Ascospores. Scale bars: D, E = 0.5 mm; F = 10 µm; G = 20 µm 20; H–Q = 10 µm.

Pi, 2021MLB60 (**holotype** GMB0231, ex-type culture GMBC0231; **isotype** KUN-HKAS 129507).

Ex-holotype strains: ITS = PQ278773, LSU = PQ278819, *rpb2* = PQ273649, *TUB2* = PQ273684.

Additional material examined: **China**, Yunnan Province, Baoshan City, Wayao Town, 25°32'14.15"N, 99°28'50.98"E, subtropical forest, on dead wood, 3 Aug. 2021, *Y.H. Pi*, 2021WYZ223 (**paratype** GMB0459, culture GMBC0459).

Notes: In the initial blast result, *Annulohypoxylon liboense* was found closely related to *A. fulvum*, but the latter can be easily differentiated by its characterizing features: stromatal surface fawn (87), KOH-extractable pigments isabelline (65) to fawn (87), and ascospores dark brown to blackish brown, averaging 10.6 × 5 µm (Fournier & Lechat 2016).

Annulohypoxylon annulatum and *A. truncatum* likewise feature dull black stromata with truncatum-type ostiolar discs and greenish olivaceous (90) to dull green (70) KOH-extractable pigments (Fournier & Lechat 2016, Kuhnert *et al.* 2017). *Annulohypoxylon annulatum* is characterized by hemispherical stromata, 2.5–5 mm thick, surface blackish brown with olivaceous tones, inconspicuous perithecial mounds, ostioles encircled by a convex disc of 0.2–0.5 mm diam., ascospores 8–11 × 4–6 µm, whereas *A. truncatum* is characterized by effused-pulvinate to glomerate stromata with conspicuous perithecial mounds up to 1/2 exposed and concave ostiolar discs 0.3–0.4 mm diam., dark brown mature stromata with reddish tones, ascospores 9–12 × 4–6 µm (Kuhnert *et al.* 2017). These characteristics differentiate both from *A. liboense.*

Annulohypoxylon liboense has a similar ascospore range to *A. elevatidiscum* but the latter has a smaller convex ostiolar disc (0.2–0.3 mm diam.) raised above the rims, larger perithecia (400–500 µm) and shorter asci (110–130 µm) with apical ring faintly bluing at the base or not bluing in Melzer's reagent (Ju & Rogers 1996, Ju *et al.* 2004). Morphologically, *Annulohypoxylon liboense* is also similar to *A. squamulosum*, but the latter differs by having a surface with a conspicuously reticulate and cracked outermost layer, ostiolar disc 0.1–0.2 mm diam., and ascospores 7–8.5 × 3–4 µm (Hsieh *et al.* 2005).

Annulohypoxylon limushanense H.M. Hu, K. Habib & Q.R. Li, ***sp. nov.*** MB 855590. Fig. 8.

Etymology: Refers to the locality of the type, Limushan Nature Reserve.

Sexual morph: *Stromata* on the surface of dead wood effused-pulvinate, separate to confluent into larger compound stromata, with inconspicuous perithecial mounds, surface pale grey (120) to dark grey (121), 5–10 cm long, 1.7–2 cm wide, 0.3–0.4 mm high, tissue below the perithecial layer black; with 10 % KOH extractable pigments dull green (70). *Perithecia* 162–178 µm high ($\bar{x}$ = 155 × 170 µm, *n* = 20), ovoid spherical, 120–200 µm wide, ostioles globose papillate, encircled with a white disc, 0.13–0.18 mm diam. *Asci* 67–78 × 3.5–4.2 µm ($\bar{x}$ = 73 × 4 µm, *n* = 30), 8-spored, unitunicate, cylindrical, short-stipitate, the stipes 20–40 µm long ($\bar{x}$ = 35 µm, *n* = 30), the spore-bearing parts 47–69 µm long ($\bar{x}$ = 55 µm, *n* = 30), with apical apparatus bluing in Melzer's reagent, discoid, inconspicuous. *Ascospores* 5–6 × 2.1–2.9 µm ($\bar{x}$ = 5.6 × 2.4 µm, *n* = 30), uniseriate, unicellular, brown, inequilateral ellipsoid, with narrowly rounded ends, with conspicuous straight germ slit covering the full spore length on the flattened side, perispore dehiscent in 10 % KOH, smooth with thickening on the flattened side, epispore smooth. *Asexual morph* not observed.

Secondary metabolites: Stromata contain truncatone A, truncatone C, and stygin according to the MS/MS analysis.

Typus: **China**, Hainan Province, Qiongzhong County, Limushan Nature Reserve, 19°12'28.95"N, 109°50'21.74"E, subtropical forest, on dead wood, 12 Nov. 2020, *Y.H. Pi*, 2020QZ131 (**holotype** GMB0479, isotype KUN-HKAS 129503).

Barcodes: ITS = PQ278761, LSU = PQ278805, *rpb2* = PQ273635, *TUB2* = PQ273670.

Additional material examined: **China**, Hainan Province, Qiongzhong County, Limushan Nature Reserve, 19°12'28.95"N, 109°50'21.74"E, subtropical forest, on dead wood, 12 Nov. 2020, *Y.H. Pi*, 2020QZ132 (**paratype** GMB0480, culture GMBC0480).

Notes: Phylogenetically, *Annulohypoxylon limushanense* is closely related to *A. atroroseum* and shares several morphological characteristics, such as similar morphology, size of ascospores and the position of the germ slit, as well as green KOH-extractable pigments. However, the new taxon can be easily differentiated by the colour of its stromata which range from surface pale grey (120) to dark grey (121) (compared to the livid purple (61), pale vinaceous grey (115) surface of young stromata and the dull black surface of mature stromata in *A. atroroseum*) (Fournier & Lechat 2016, Kuhnert *et al.* 2017). Furthermore, *A. atroroseum* typically has larger perithecia (0.3–0.5 mm) with truncatum or bovei-type ostiolar discs often featuring irregular rims (Fournier & Lechat 2016, Kuhnert *et al.* 2017), whereas the new taxon has smaller perithecia (120–200 µm wide × 162–178 µm high) with white ostiolar discs that are globose and papillate. In terms of anatomical features and KOH-extractable pigment, it also shows resemblance to *A. stygium*. However, the latter species exhibits stromatal surface colours ranging from fugacious dark brick (60) to dark vinaceous (82), and mature stromata are black. Its perithecia measure 0.3–0.35 mm diam. and feature truncatum- or bovei-type ostiolar discs, which are sometimes overlain by white granular tissue (Fournier & Lechat 2016, Kuhnert *et al.* 2017).

Annulohypoxylon maolanense K. Habib, Y.H. Pi & Q.R. Li, ***sp. nov.*** MB 855591. Fig. 9.

Etymology: Refers to the place of collection, Maolan National Nature Reserve.

Sexual morph: *Stromata* on the surface of dead branches effused-pulvinate, separate to confluent into larger compound stromata, with inconspicuous perithecial mounds, surface mouse grey (118) to brown vinaceous (84), carbonaceous,

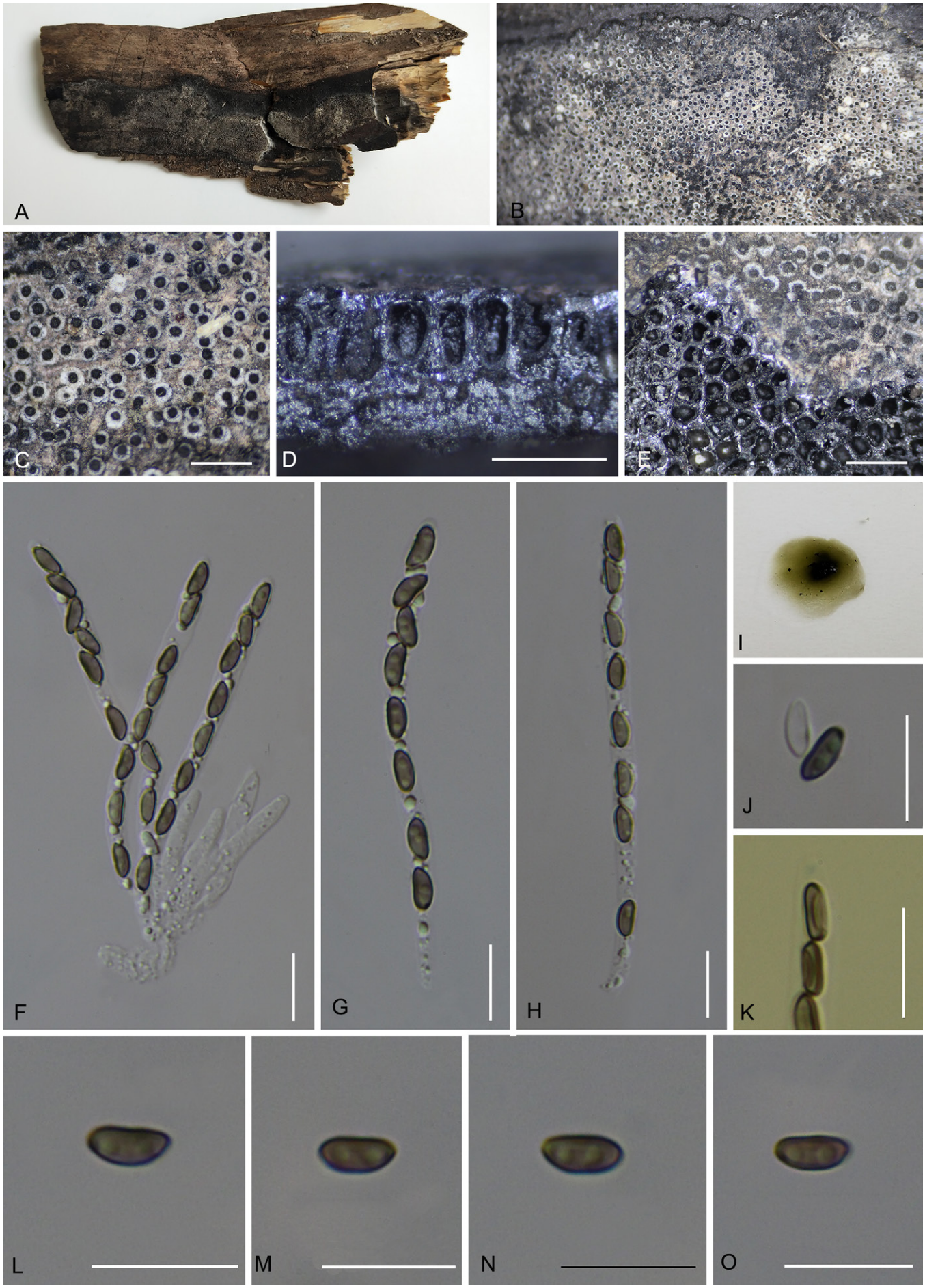

Fig. 8. *Annulohypoxylon limushanense* (GMB0479, holotype). **A.** Stromatal habit on wood. **B.** Stromatal surface. **C.** Ostioles and ostiolar discs. **D.** Longitudinal section of the stromata showing perithecia. **E.** Transverse section of stromata showing perithecia. **F–H.** Asci in distilled water. **I.** Stromatal KOH-extractable pigment. **J.** Perispore dehiscent in 10 % KOH. **K.** Ascal apical apparatus (stained in Melzer's reagent). **L–O.** Ascospores. Scale bars: C–E = 0.5 mm; F–H, J–O = 10 µm.

Fig. 9. *Annulohypoxylon maolanense* (GMB0232, holotype). **A.** Stromatal habit on wood. **B.** Stromatal surface. **C.** Ostioles and ostiolar discs. **D.** Transverse section of stromata. **E.** Longitudinal section of the stromata showing perithecia. **F–I.** Asci in distilled water. **J.** Stromatal KOH-extractable pigment. **K.** Perispore dehiscent in 10 % KOH. **L.** Ascal apical apparatus (not bluing in Melzer's reagent). **M, N.** Ascospores. **O, P.** Colonies on OA (O-upper, P-lower). Scale bars: C–E = 0.5 mm; F–I, K–N = 10 µm.

1–6 cm long, 0.6–1.6 cm wide, 0.5–0.7 mm high, tissue below the perithecial layer black; with 10 % KOH extractable pigments dull green (70). *Perithecia* obovoid, 250–360 µm wide, 300–350 µm high ($\bar{x}$ = 308 × 335 µm, *n* = 20), ostioles conical papillate, encircled with a truncatum-type disc, 0.15–0.2 mm diam. *Asci* 80–106 × 3–5 µm ($\bar{x}$ = 95 × 4 µm, *n* = 30), 8-spored, unitunicate, cylindrical, long-stipitate, the stipes 20–40 µm ($\bar{x}$ = 25 µm, *n* = 30) long, the spore-bearing parts 55–65 µm long ($\bar{x}$ = 60 µm, *n* = 30), apical apparatus not bluing in Melzer's reagent. *Ascospores* 6–7 × 2.8–3.5 µm ($\bar{x}$ = 6.5 × 3 µm, *n* = 30), uniseriate, unicellular, inequilateral ellipsoid, with narrowly rounded ends, brown, with inconspicuous slightly curved germ slit covering the full spore length on flattened side, perispore dehiscent in 10 % KOH, smooth with a thickening on flattened side, epispore smooth. *Asexual morph* not observed.

Culture characteristics: Colonies on OA reaching the edge of the Petri dish 5 cm in 3 wk, surface white, cotton-like, flocculent, with black raised spots; reverse edges white, black or dark slate blue (111) at the middle part. Not sporulating on OA nor on PDA.

Secondary metabolites: Stromata contain truncatone A, truncatone C, and stygin according to the MS/MS analysis.

Typus: **China**, Guizhou Province, Qiannan Buyi and Miao Autonomous Prefecture, Libo County, Maolan National Nature Reserve, 25°18'2.76"N, 108°4'29.48"E, subtropical moist broad leaf forest, on branch of *Quercus* sp., 9 Jul. 2021, *Y.H. Pi*, 2021MLB53 (**holotype** GMB0232, ex-type culture GMBC0232; **isotype** KUN-HKAS 129508).

Barcodes: ITS = PQ278764, LSU = PQ278808, *rpb2* = PQ273638, *TUB2* = PQ273673.

Additional material examined: **China**, Yunnan Province, Changning County, Lancang River Nature Reserve, 25°01'28.12"N, 99°36'77.47"E, subtropical forest, on dead wood, 5 Oct. 2019, *Y.H. Pi*, 2019LC032 (**paratype** GMB0458, culture GMBC0458).

Notes: Morphologically, *A. maolanense* is similar to *A. stygium* with features such as similar-sized ostiolar discs and greenish olivaceous (90) to dull green (70) KOH-extractable pigments. However, the latter has larger perithecia (0.3–0.5 mm) and the colour of the stromata surface is fugacious dark brick (60) to dark vinaceous (82), maturing to black, with ascospores averaging 5.5 × 2.5 µm (Ju *et al*. 1996, Fournier & Lechat 2016, Kuhnert *et al.* 2017).

Phylogenetically, it is closely related to *A. atroroseum* and shares several morphological characteristics, such as similar stromatal morphology and size of ascospores, as well as green KOH-extractable pigments. However, the new taxon can be easily differentiated by the colour of its stromata being mouse grey (118) to brown vinaceous (84) (compared to the livid purple (61), pale vinaceous grey (115) surface of young stromata and the dull black surface of mature stromata in *A. atroroseum*) (Fournier & Lechat 2016, Kuhnert *et al.* 2017). Furthermore, *A. atroroseum* typically has larger perithecia (0.3–0.5 mm) with truncatum- or bovei-type ostiolar discs often featuring irregular rims (Fournier & Lechat 2016, Kuhnert *et al.* 2017). Morphologically, it also resembles the newly described species *A. olivaceogriseum* which is differentiated by its olivaceous grey (121) stromata, and smaller ascospores (5.5–6.5 × 2–3 µm).

Annulohypoxylon microdiscum (Y.M. Ju & J.D. Rogers) Sir & Kuhnert, *Fungal Diversity* **85**: 24. 2016. MB 552345. Fig. 10.

Basionym: *Hypoxylon moriforme* var. *microdiscus* Y.M. Ju & J.D. Rogers *Mycol. Mem.* **20**: 217. 1996.

Synonym: *Annulohypoxylon moriforme* var. *microdiscum* (Y.M. Ju & J.D. Rogers) Y.M. Ju *et al.* [as '*microdiscus*'], *Mycologia* **97**: 859. 2005.

Sexual morph: *Stromata* on the surface of dead wood spherical, effused to effused-pulvinate, with perithecial mounds conspicuous to less than 1/4 exposed, surface black, carbonaceous, 0.7–2.3 cm long, 0.3–0.7 cm wide, 0.4–0.6 mm thick ($\bar{x}$ = 1.8 cm × 0.62 cm × 0.54 mm, *n* = 10), brownish granules between perithecia, with 10 % KOH extractable pigments umber (9). *Perithecia* 326–400 µm wide, 256–380 µm high ($\bar{x}$ = 380 × 355 µm, *n* = 20), spherical, ostioles papillate, black, with a truncatum-type disc, 0.14–0.16 mm diam. *Asci* 95–110 × 5.5–6.5 µm ($\bar{x}$ = 102 × 6 µm, *n* = 30), 8-spored, unitunicate, cylindrical, long-stipitate, the stipes 30–55 µm long ($\bar{x}$ = 44 µm, *n* = 30), the spore-bearing parts 75–85 µm long ($\bar{x}$ = 80 µm, *n* = 30), apical apparatus not bluing in Melzer's reagent. *Ascospores* 9–11 × 4–5 µm ($\bar{x}$ = 10 × 4.5 µm, *n* = 30), uniseriate, unicellular, inequilateral ellipsoidal with narrowly rounded ends, brown to dark brown, with conspicuous straight germ slit covering the full spore length on the convex side, perispore dehiscent in 10 % KOH, smooth with a thickening on the convex side, epispore smooth. *Asexual morph* not observed.

Culture characteristics: Colonies on OA reaching the edge of the Petri dish 5 cm in 3 wk, surface white, cottony, flocculent, irregular; reverse side flesh (37) to greyish sepia (106), colony. Not sporulating on OA nor on PDA.

Secondary metabolites: Stromata contain different so far unknown metabolites according to the MS/MS analysis.

Materials examined: **China**, Yunnan Province, Xishuangbannan Nature Reserve, 22°17'35.40"N, 100°55'57.17"E, subtropical forest, on dead branch of unknown plant, 8 Aug. 2021, *Y.H. Pi*, 2021XSBN23 (GMB0233, culture GMBC0233); Yunnan Province, Xishuangbannan Primeval Forest Park, 22°32'48.71"N, 100°40'19.15"E, on dead branch of unknown plant, 10 Aug. 2021, *Y.H. Pi*, 2021XSBNY5 (GMB0234, culture GMBC0234).

Notes: Kuhnert *et al.* (2017) elevated the variety *A. moriforme* var. *microdiscum* to species level based on evidence from phylogenetic, chemotaxonomic, and morphological data. Morphologically, *A. microdiscum* differs from *A. moriforme* by having much smaller ostiolar discs, blackish granules mixed with orange ones around the perithecia, pale umber (9) KOH-extractable pigments, and an inamyloid apical ring (Kuhnert *et al*. 2017). Chemical analysis can easily separate *A. moriforme* from *A. microdiscum* by the presence of truncatones A and C, which are lacking in *A. microdiscum* (Kuhnert *et al*. 2017).

Fig. 10. *Annulohypoxylon microdiscum* (GMB0233). **A.** Stromatal habit on wood. **B.** Stromatal surface. **C.** Ostioles and ostiolar discs. **D.** Longitudinal section of the stromata showing perithecia. **E.** Transverse section of stromata showing perithecia. **F–H.** Asci in distilled water. **I.** Stromatal KOH-extractable pigment. **J.** Perispore dehiscent in 10 % KOH. **K.** Ascal apical apparatus (not bluing in Melzer's reagent). **L, M.** Ascospores showing germ slit. **N, O.** Culture on OA (N-upper, O-lower). Scale bars: D, E = 0.5 mm; F–H, J–M = 10 µm.

The sequences from our collections closely match those of *A. microdiscum* YMJ90080807, showing 99 % similarity in the beta-tubulin gene. Phylogenetically, they also cluster together, and phenotypically show the same morphological characteristics (Kuhnert *et al*. 2017). This is the first report of *A. microdiscum* from Southwestern China.

Annulohypoxylon olivaceogriseum Y.H. Pi, K. Habib & Q.R. Li, ***sp. nov.*** MB 855592. Fig. 11.

Etymology: Refers to the olivaceous grey colour of the stromatal surface.

Sexual morph: *Stromata* on the surface of dead wood, effused-pulvinate, separate to confluent into larger compound stromata, with inconspicuous perithecial mounds, surface olivaceous grey (121), 1–6 cm long, 0.7–1.5 cm wide, 0.5–0.6 mm high ($\bar{x}$ = 3.6 cm × 1 cm × 0.55 mm, *n* = 10), tissue below the perithecial layer black; with 10 % KOH extractable pigments dull green (70). *Perithecia* 213–302 µm wide, 240–373 µm high ($\bar{x}$ = 265 × 335 µm, *n* = 20), obovoid, ostioles conical papillate, encircled with a truncatum-type disc, 0.2-0.3 mm diam. *Asci* 90–100 × 3.5–4 µm ($\bar{x}$ = 95 × 3.8 µm, *n* = 30), 8-spored, unitunicate, cylindrical, long-stipitate, the stipes 20–40 µm long ($\bar{x}$ = 35 µm, *n* = 30), the spore-bearing parts 60–70 µm long ($\bar{x}$ = 65 µm, *n* = 30), with apical apparatus bluing in Melzer's reagent, discoid, inconspicuous. *Ascospores* 5.5–6.5 × 2–3 µm ($\bar{x}$ = 6 × 2.5 µm, *n* = 30), uniseriate, unicellular, ellipsoid, inequilateral, with narrowly rounded ends, brown, with inconspicuous straight germ slit covering the full spore length on the flattened side, perispore dehiscent in 10 % KOH, smooth with a thickening on flattened side, epispore smooth. *Asexual morph* not observed.

Culture characteristics: Colonies on OA reaching the edge of the Petri dish 5 cm in 3 wk, surface white, cotton-like, flocculent, round, with black raised shiny dots; reverse ochreous (44) to apricot (42), with a black or dark cyan blue (27) strip in the centre. Not sporulating on OA nor on PDA.

Secondary metabolites: Stromata contain truncatone A, truncatone C, and stygin according to the MS/MS analysis.

Typus: **China**, Guizhou Province, Rongjiang County, Leigong Mountain Nature Reserve, 26°04'21.93"N, 108°19'16.53"E, tropical forest, on dead wood, 28 Aug. 2020, *Y.H. Pi*, 2020LGS195 (**holotype** GMB0230, ex-type culture GMBC0230; **isotype** KUN-HKAS 129512).

Barcodes: ITS = PQ278766, LSU = PQ278810, *rpb2* = PQ273640, *TUB2* = PQ273675.

Additional material examined: **China**, Guizhou Province, Rongjiang County, Leigong Mountain Nature Reserve, 26°22'53.19"N, 108°21'49.74"E, tropical forest, on dead wood, 28 Aug. 2020, *Y.H. Pi*, 2020LGS56 (**paratype** GMB0448, culture GMBC0448).

Notes: Morphologically, *A. olivaceogriseum* resembles *A. stygium* in ascospore morphology, size, and KOH pigmentation. However, they differ in that *A. olivaceogriseum* has larger perithecia (0.3–0.5 mm) with small ostiolar discs < 0.2 mm diam. (vs 0.2–0.3 mm diam.), and smaller asci 60–80 µm in total length with 45–48 µm spore-bearing parts (compared to 90–100 µm in total length with 60–70 µm spore-bearing parts). Additionally, the colour of the stromatal surface in *A. stygium* is fugacious dark brick (60) to dark vinaceous (82), mature black (Ju *et al*. 1996, Fournier & Lechat 2016, Kuhnert *et al.* 2017).

Morphologically, it is also confused with *A. atroroseum* in ascospore morphology, size, and green KOH pigments. However, the new taxon can be easily differentiated by the colour of its stromatal surface which is olivaceous grey (121) [compared to the livid purple (61), pale vinaceous grey (115) surface of young stromata and the dull black surface of mature stromata in *A. atroroseum*] (Fournier & Lechat 2016, Kuhnert *et al.* 2017). Furthermore, *A. atroroseum* typically has larger perithecia (0.3–0.5 mm) with smaller (0.15–0.2 mm) ostiolar discs (Fournier & Lechat 2016, Kuhnert *et al.* 2017).

Annulohypoxylon pseudoalbidiscum Y.H. Pi, K. Habib & Q.R. Li, ***sp. nov.*** MB 855593. Fig. 12.

Etymology: Refers to the similar species, *Annulohypoxylon albidiscum*.

Sexual morph: *Stromata* on the surface of dead branches effused-pulvinate, separate to confluent into larger compound stromata, with perithecial mounds 1/3 exposed, surface rough, black, carbonaceous, 1.3–2 cm long, 0.2–0.7 cm wide, 0.3–0.4 mm high ($\bar{x}$ = 1.7 cm × 0.45 cm × 0.35 mm, *n* = 8), tissue below the perithecial layer black; with 10 % KOH extractable pigments dull green (70). *Perithecia* 280–500 µm diam. ($\bar{x}$ = 380 ***µm,*** *n* = 20), spherical, *ostioles* conical papillate, encircled with a truncatum-type disc, 0.12–0.15 mm diam. *Asci* 80–105 × 4.5–6 µm ($\bar{x}$ = 85 × 5.2 µm, *n* = 30), 8-spored, unitunicate, cylindrical, short-pedicellate, the stipes 15–25 µm long ($\bar{x}$ = 20 µm, *n* = 30), the spore-bearing parts 55–64 µm long ($\bar{x}$ = 58 µm, *n* = 30), with apical apparatus bluing in Melzer's reagent, discoid, 1.3–1.8 × 0.5–0.8 µm ($\bar{x}$ = 1.5 × 0.7 µm, *n* = 20). *Ascospores* 7–8.3 × 3.5–4.5 µm ($\bar{x}$ = 7.5 × 4.2 µm, *n* = 30), uniseriate, unicellular, inequilateral ellipsoid, with broadly rounded ends, brown to dark brown, with conspicuous straight germ slit covering the full spore length on the convex side, perispore dehiscent in 10 % KOH, smooth with a thickening on the convex side, epispore smooth. *Asexual morph* not observed.

Culture characteristics: Colonies on OA reaching the edge of the Petri dish 5 cm in 3 wk, surface white, cottony, flocculent, irregular; reverse side colony, peach (4) or flesh (37). Not sporulating on OA nor on PDA.

Secondary metabolites: Stromata contain different so far unknown metabolites and truncatone A and hypoxylonol C/F according to the MS/MS analysis.

Typus: **China**, Guizhou Province, Rongjiang County, Leigong Mountain Nature Reserve, 26°04'21.93"N, 108°19'16.53"E, subtropical forest, on dead wood, 28 Aug. 2020, *Y.H. Pi*, 2020LGS153 (**holotype** GMB0235, ex-type culture GMBC0235; **isotype** KUN-HKAS 129513).

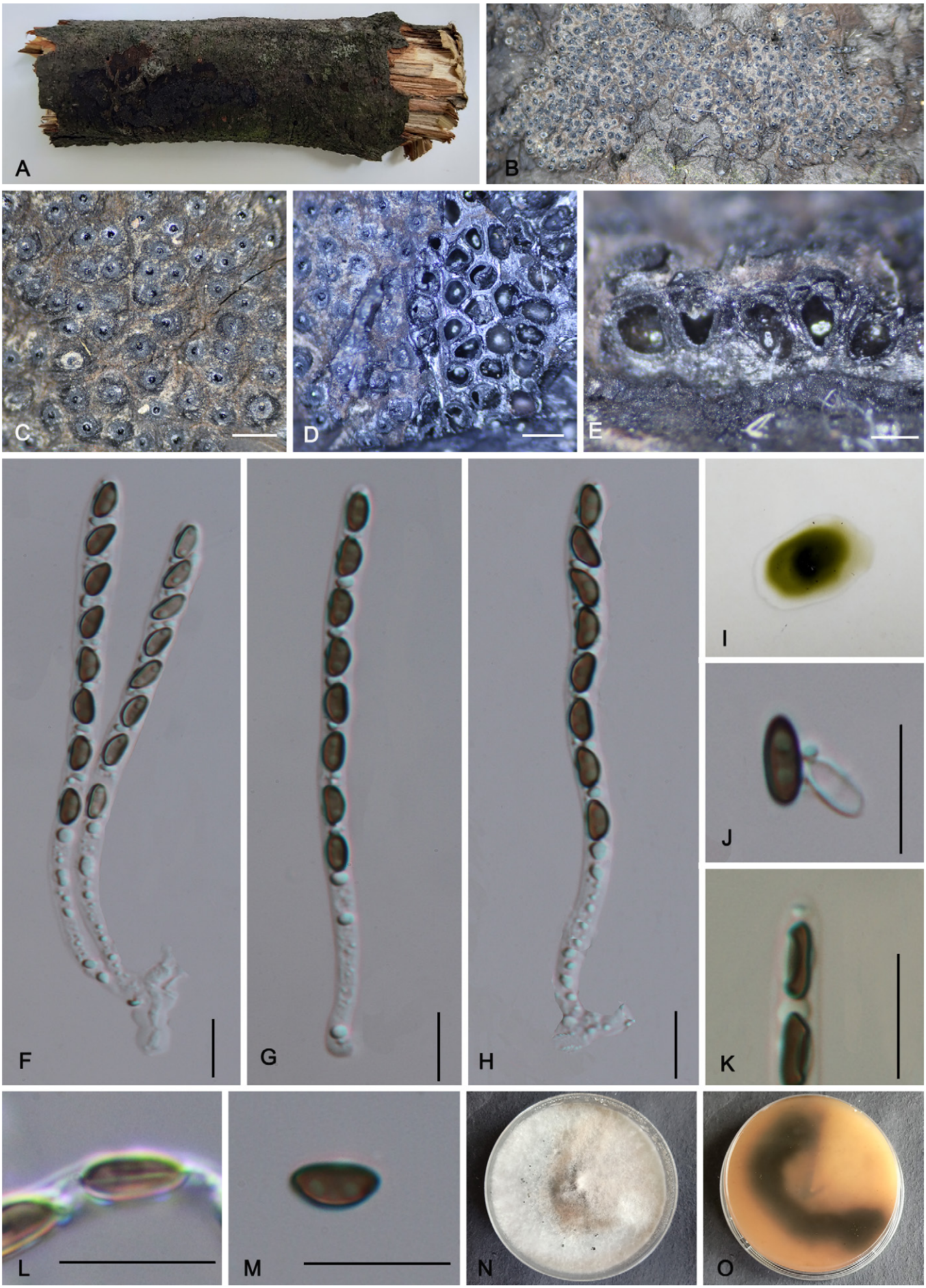

Fig. 11. *Annulohypoxylon olivaceogriseum* (GMB0230, holotype). **A.** Stromatal habit on wood. **B.** Stromatal surface. **C.** Ostioles and ostiolar discs. **D.** Transverse section of stromata showing perithecia. **E.** Longitudinal section of the stromata showing perithecia. **F–H.** Asci in distilled water. **I.** Stromatal KOH-extractable pigment. **J.** Perispore dehiscent in 10 % KOH. **K.** Ascal apical apparatus (stained in Melzer's reagent). **L, M.** Ascospores. **N, O.** Colonies on OA (N-upper, O-lower). Scale bars: C–E = 0.5 mm; F–H, J–M = 10 µm.

Fig. 12. *Annulohypoxylon pseudoalbidiscum* (GMB0235, holotype). **A.** Stromatal habit on wood. **B.** Stromatal surface. **C.** Ostioles and ostiolar discs. **D.** Transverse section of stromata showing perithecia. **E.** Longitudinal section of the stromata showing perithecia. **F–H.** Asci in distilled water. **I.** Stromatal KOH-extractable pigment. **J.** Perispore dehiscent in 10 % KOH. **K.** Ascal apical apparatus (stained in Melzer's reagent). **L, M.** Ascospores. **N, O.** Colonies on OA (N-upper, O-lower). Scale bars: C–E = 0.5 mm; F–H, J–M = 10 µm.

Barcodes: ITS = PQ278788, LSU = PQ278834, *rpb2* = PQ273664, *TUB2* = PQ273699.

Additional material examined: **China**, Guizhou Province, Rongjiang County, Leigong Mountain Nature Reserve, 26°04'21.93"N, 108°19'16.53"E, subtropical forest, on dead wood, 28 Aug. 2020, *Y.H. Pi*, 2020LGS99 (**paratype** GMB0236, culture GMBC0236).

Notes: Phylogenetically and morphologically, *A. pseudoalbidiscum* is closely related to *A. albidiscum*, exhibits similar-sized ascospores and yields the same pigmentation in KOH. However, *A. albidiscum* is distinguished by stromata with conspicuous perithecial mounds containing large perithecia 0.4–0.8 mm diam., with the ostioles surrounded by white tissue (Li et al. 2016). Moreover, *A. albidiscum* has long-pedicellate asci and ascospores with narrowly rounded ends (Li *et al.* 2016).

In terms of ascospore size and KOH pigmentation, it is also similar to *A. yungense*. However, *A. yungense* differs in having a brown vinaceous (84) to black surface colour with a brown vinaceous tone, wider perithecia (0.4–0.7 mm) with a wider disc (0.2–0.3 mm diam.), longer asci (115.5–150 µm in total length), slightly larger ascospores (8–9.2 × 3.6–4.5 µm), and perithecial mounds inconspicuous up to 2/3 exposed (Kuhnert *et al.* 2017).

Annulohypoxylon primevalense H.M. Hu, K. Habib & Q.R. Li, ***sp. nov.*** MB 855594. Fig. 13.

Etymology: Refers to the locality of the type, Primeval Forest Park.

Sexual morph: *Stromata* on the surface of dead wood effused-pulvinate, surface black with olivaceous tones formed on the outermost stromatal layer, with perithecial mounds 1/4 exposed, carbonaceous, 0.4–5 cm long, 0.2–1.7 cm wide, 0.9–1.3 mm high, tissue below the perithecial layer green to black, with 10 % KOH extractable pigments olivaceous green (90). *Perithecia* 180–350 µm wide, 260–385 µm high ($\bar{x}$ = 295 × 350 µm, *n* = 20), spherical, ostioles conical papillate, encircled with a truncatum-type disc, 0.2–0.3 mm diam. *Asci* 80–115 × 4–5 µm ($\bar{x}$ = 90.8 × 4.5 µm, *n* = 30), 8-spored, unitunicate, cylindrical, long-stipitate, the stipes 30–55 µm long ($\bar{x}$ = 45 µm, *n* = 30), the spore-bearing parts 65–78 µm long ($\bar{x}$ = 70 µm, *n* = 30), with apical apparatus bluing in Melzer's reagent, discoid, inconspicuous. *Ascospores* 6–8 × 2.5–3.5 µm ($\bar{x}$ = 6.9 × 3.1 µm, *n* = 30), uniseriate, unicellular, inequilateral to almost equilateral ellipsoid, with rounded ends, brown, with straight germ slit covering the full spore length on the convex side, perispore dehiscent in 10 % KOH, with a thickening on the convex side, epispore smooth. *Asexual morph* not observed.

Culture characteristics: Colonies on OA reaching the edge of the Petri dish 5 cm in 3 wk, azonate, surface white, felty, cottony, with scattered black patches, forming a rosy vinaceous (58) circular ring in the middle; reverse dark mouse grey (119) to fuscous black (104), peach (4) at edges. Not sporulating on OA nor on PDA.

Secondary metabolites: Stromata contain several yet unknown azaphilone-like compounds and other fatty acid-like molecules according to the MS/MS analysis.

Typus: **China**, Yunnan Province, Xishuangbanna Primeval Forest Park, 22°32'48.61"N, 100°40'19.25"E, tropical forest, on dead wood, 10 Aug. 2021, *Y.H. Pi*, 2021XSBNY2 (**holotype** GMB0240, ex-type culture GMBC0240; **isotype** KUN-HKAS 129524).

Barcodes: LSU = PQ278814, *rpb2* = PQ273644, *TUB2* = PQ273679.

Additional material examined: **China**, Hainan Province, Baisha County, Yingge Ling National Nature Reserve, 19°13′23.10″N, 109°15′12.30″E, subtropical forest, on dead wood of an unknown plant, 18 Jul. 2022, *H.M. Hu*, 2022YGL2 (**paratype** GMB4207).

Notes: Initial blast result of ITS and *TUB2* sequences from *Annulohypoxylon primevalense* showed the highest similarity to *A. viridistratum*. In the phylogram (Fig. 2), the two species formed a well-supported sister relationship. Morphologically, it closely resembles *A. viridistratum* in stromatal surface colouration. However, the new taxon differs in having smaller perithecia 180–350 µm wide (vs 0.3–0.5 mm diam.), asci with short stipes 30–55 µm (vs 33–84 µm long), and larger ascospores 6–8 × 2.5–3.5 µm (vs 5.7–6.8 × 2.4–3 µm). The shiny stromatal surface of *A. primevalense* is reminiscent of *A. nitens*, but the latter differs in having larger perithecia (0.4–1.2 mm diam.) with large ostiolar discs (0.2–0.5 mm) and larger ascospores (6.5–11 × 3–4.5 µm) (Kuhnert *et al*. 2017). Additionally, the new taxon has a layer of green tissue mixed with black tissue below the perithecia, a feature previously observed only in *A. viridistratum.*

Annulohypoxylon rongjiangense Y.H. Pi, K. Habib & Q.R. Li, ***sp. nov.*** MB 855596. Fig. 14.

Etymology: Refers to the locality of the type specimen, Rongjiang County.

Sexual morph: *Stromata* on the surface of decaying wood, effused-pulvinate rarely glomerate, scattered, separate to confluent into larger compound stromata, with perithecial mounds 1/2 exposed, surface leaden grey (112) or leaden black (126), carbonaceous, 0.5–2.5 cm long, 0.3–1.1 cm wide, 1–1.5 mm high ($\bar{x}$ = 1.4 cm × 0.5 cm × 1.2 mm, *n* = 10), tissue below the perithecial layer black, with 10 % KOH extractable pigments dull green (70). *Perithecia* 430–600 µm wide, 400–570 µm high ($\bar{x}$ = 535 × 473 µm, *n* = 20), spherical, ostioles conical papillate, encircled with a truncatum-type disc, 0.25–0.35 mm diam. *Asci* 95–120 × 5.5–8 µm ($\bar{x}$ = 108 × 6.5 µm, *n* = 30), 8-spored, unitunicate, cylindrical, long-stipitate, the stipes 30–55 µm long ($\bar{x}$ = 40 µm, *n* = 30), the spore-bearing parts 65–75 µm long ($\bar{x}$ = 69 µm, *n* = 30), apical apparatus not bluing in Melzer's reagent. *Ascospores* 7–9 × 3.5–5.5 µm ($\bar{x}$ = 8 × 4.5 µm, *n* = 30), uniseriate, unicellular, ellipsoid, slightly inequilateral to almost equilateral, with broadly rounded ends, brown to dark brown, with fairly conspicuous straight germ slit

Fig. 13. *Annulohypoxylon primevalense* (GMB0240, holotype). **A.** Stromatal habit on wood. **B.** Stromatal surface. **C.** Ostioles and ostiolar discs. **D.** Transverse section of stromata showing perithecia. **E.** Longitudinal section of the stromata showing perithecia. **F–H.** Asci in distilled water. **I.** Stromatal KOH-extractable pigment. **J.** Perispore dehiscent in 10 % KOH. **K.** Ascal apical apparatus (stained in Melzer's reagent). **L, M.** Ascospores. **N, O.** Colonies on OA (N-upper, O-lower). Scale bars: D, E = 0.5 mm; F–H, J–M = 10 µm.

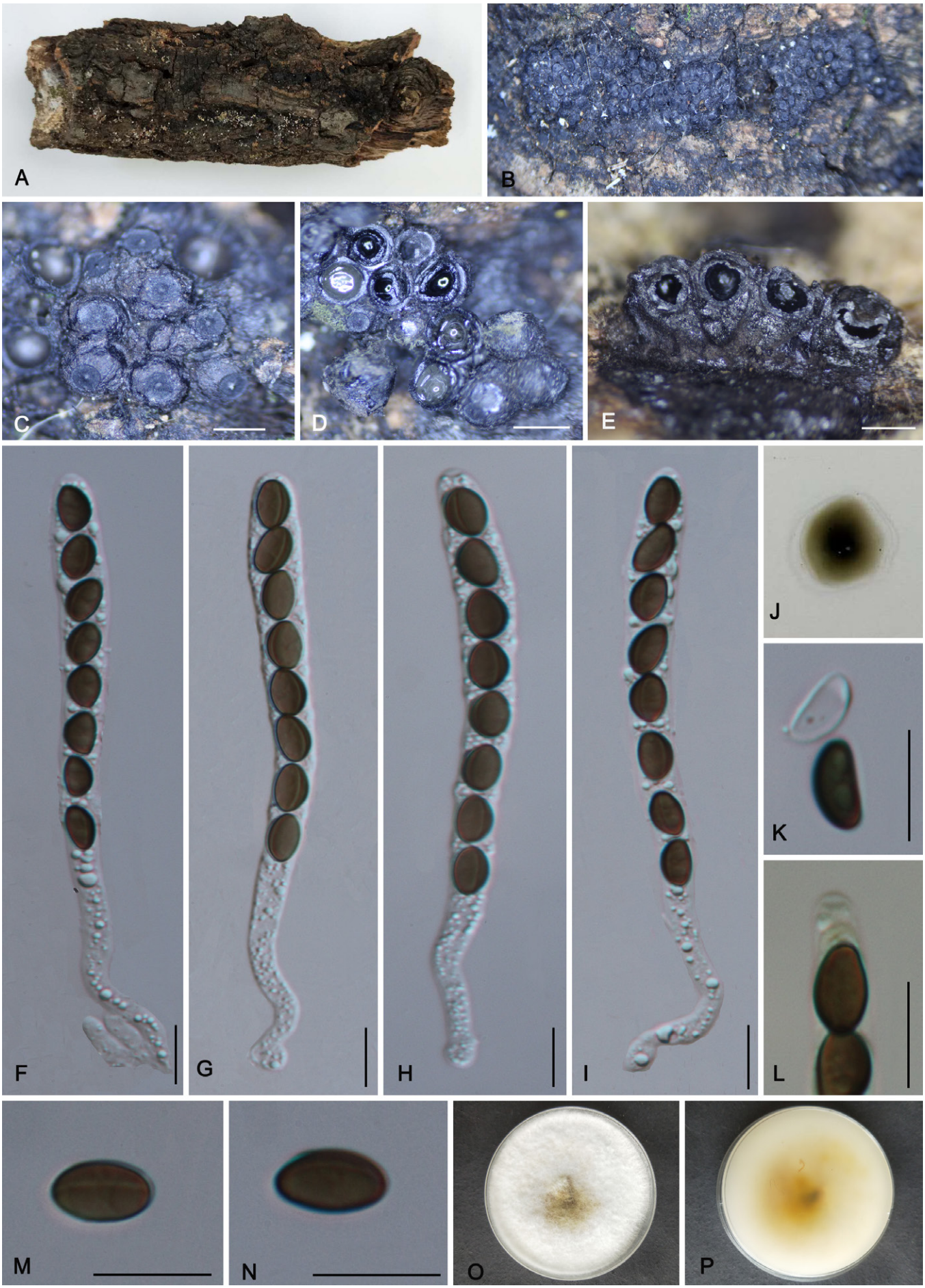

Fig. 14. *Annulohypoxylon rongjiangense* (GMB0229, holotype). **A.** Stromatal habit on wood. **B.** Stromatal surface. **C.** Ostioles and ostiolar discs. **D.** Transverse section of stromata showing perithecia. **E.** Longitudinal section of the stromata showing perithecia. **F–I.** Asci in distilled water. **J.** Stromatal KOH-extractable pigment. **K.** Perispore dehiscent in 10 % KOH. **L.** Ascal apical apparatus (non-bluing in Melzer's reagent). **M, N.** Ascospores. **O, P.** Colonies on OA (O-upper; P-lower). Scale bars: C–E = 0.5 mm; F–I, K–N = 10 µm.

covering the full spore length on the convex side, perispore dehiscent in 10 % KOH, smooth with a thickening on the convex side, epispore smooth. *Asexual morph* not observed.

Culture characteristics: Colonies on OA reaching the edge of the Petri dish 5 cm in 3 wk, surface white, cottony, circular, flocculent or velvety, dense; reverse white, luteous (12) to cinnamon (62) at centre. Not sporulating on OA nor on PDA.

Secondary metabolites: Stromata contain truncatone A, stygin, and related congeners as major metabolites according to the MS/MS analysis.

Typus: **China**, Guizhou Province, Rongjiang County, Leigong Mountain Nature Reserve, 26°04'21.93"N, 108°19'16.53"E, subtropical forest, on dead wood, 28 Aug. 2020, *Y.H. Pi*, 2020LGS20 (**holotype** GMB0229, ex-type culture GMBC0229; **isotype** KUN-HKAS 129514).

Barcodes: ITS = PQ278780, LSU = PQ278826, *rpb2* = PQ273656, *TUB2* = PQ273691.

Additional materials examined: **China**, Guizhou Province, Rongjiang County, Leigong Mountain Nature Reserve, 26°4'8.53"N, 108°19'5.44"E, subtropical forest, on dead wood, 28 Aug. 2020, *Y.H. Pi*, 2019LGS7 (**paratype** GMB0441, culture GMBC0441); Guizhou Province, Rongjiang County, Leigong Mountain Nature Reserve, 26°20'30.23"N, 108°17'20.90"E, subtropical forest, on dead wood, 29 Aug. 2020, *Y.H. Pi*, 2019LGS124 (GMB0442, culture GMBC0442); Guizhou Province, Rongjiang County, Leigong Mountain Nature Reserve, 26°21'48.77"N, 108°6'8.51"E, subtropical forest, on dead wood, 29 Aug. 2020, *Y.H. Pi*, 2019LGS200 (GMB0443, culture GMBC0443).

Notes: Phylogenetically, *A. rongjiangense* formed a well-supported sister clade with *A. viridipigmentum*. Morphologically, they also closely resemble each other, but *A. viridipigmentum* differs in having inequilateral ellipsoidal spores with narrowly rounded ends, slightly narrower ascospores (3.3–4.5 µm), larger asci 125–140 × 5–6.5 µm with long stipes 45–70 µm, and an apical apparatus does not turn blue in Melzer's reagent.

In the initial blast result, *A. rongjiangense* was found to be more closely related to *A. areolatum*, and phylogenetically also clustered in same clade. However, *A. areolatum* can be easily differentiated by having smaller stromata (1–5.5 mm diam.), usually containing only up to 10 perithecia, larger ostiolar discs 0.3–0.7 mm diam., stromata surface colour ranging from sepia (116) to grey olivaceous (107), and larger asci 121–181 µm in total length (Kuhnert *et al.* 2017).

Among species with greenish KOH-extractable pigments and similar ascospore sizes that can be confused with *A. rongjiangense*, *A. moriforme* differs by having larger perithecia (0.4–0.8 mm diam.) and ostiolar discs (0.2–0.4 mm) and frequently pulvinate to glomerate stromata, and *A. microcarpum* differs by having smaller perithecia, 0.15–0.2 mm diam. and ostiolar discs 0.1 mm diam. (Fournier *et al*. 2010).

Annulohypoxylon subbahnphadengense Y.H. Pi, K. Habib & Q.R. Li, ***sp. nov.*** MB 855597. Fig. 15.

Etymology: Refers to *Annulohypoxylon bahnphadengense*, which is morphologically similar.

Sexual morph: *Stromata* on the surface of dead wood glomerate, effused-pulvinate, with the tendency to be perithecioid but joined by very thin stromatal tissue, usually confluent, with perithecial mounds 1/2 exposed, surface black, carbonaceous, 0.6–3.5 cm long, 1–2.4 cm wide, 0.5–0.6 mm high ($\bar{x}$ = 2 cm × 1 cm × 0.6 mm, *n* = 10), tissue below the perithecial layer brown to black; with 10 % KOH extractable pigments Isabelline (65) to greyish sepia (106). *Perithecia* 500–800 µm diam. ($\bar{x}$ = 640, *n* = 20), spherical, ostioles conical papillate, encircled with a truncatum-type disc, 0.22–0.3 mm diam. *Asci* 110–143 × 4–5.8 µm ($\bar{x}$ = 130 × 5 µm, *n* = 30), 8-spored, unitunicate, cylindrical, long-stipitate, the stipes 47–65 µm long ($\bar{x}$ = 56 µm, *n* = 30), the spore-bearing parts 50–72 µm long ($\bar{x}$ = 63 µm, *n* = 30), apical apparatus bluing in Melzer's reagent, discoid, 1–1.2 × 0.4–0.6 µm ($\bar{x}$ = 1.1 × 0.5 µm, *n* = 20). *Ascospores* 6–7 × 2.9–3.7 µm ($\bar{x}$ = 6.6 × 3.3 µm, *n* = 30), uniseriate, unicellular, inequilateral ellipsoid with narrowly rounded ends, brown, with a faint straight germ slit covering the full spore length on the convex side, perispore dehiscent in 10 % KOH, smooth with a thickening on the convex side, epispore smooth. *Asexual morph* not observed.

Culture characteristics: Colonies on OA reaching the edge of the Petri dish 5 cm in 3 wk, azonate, surface white, velvety to felty, irregular at margin; reverse dark livid (80). Not sporulating on OA nor on PDA.

Secondary metabolites: Stromata contain several unknown metabolites, as well as truncatone A and hinnulin A according to the MS/MS analysis.

Typus: **China**, Hainan Province, Wuzhishan City, Atuoling Forest Park, 18°48'26.79"N, 109°30'55.47"E, subtropical broadleaf forest, on dead wood, 15 Nov. 2020, *Y.H. Pi & Q.R. Li*, 2020ATL11 (**holotype** GMB0469, ex-type culture GMBC0469; **isotype** KUN-HKAS 129518).

Barcodes: ITS = PQ278775, LSU = PQ278821, *rpb2* = PQ273651, *TUB2* = PQ273686.

Additional materials examined: **China**, Hainan Province, Wuzhishan City, Atuoling Forest Park, 18°48'26.79"N, 109°30'55.47"E, subtropical broadleaf forest, on dead wood, 15 Nov. 2020, *Y.H. Pi & Q.R. Li*, 2020ATL2 (**paratype** GMB0470, culture GMBC0470); Hainan Province, Qiongzhong County, Limushan Nature Reserve, 19°12'28.95"N, 109°50'21.74"E, subtropical forest, on dead wood, 12 Nov. 2020, *Y.H. Pi*, 2020QZ49 (GMB0471, culture GMBC0471).

Notes: In the phylograms (Fig. 2), the sequences of *A. subbahnphadengense* formed a well-supported sister clade with *A. bahnphadengense* STMA13115 and *A. nouraguense* MUCL54607. Morphologically also, *A. subbahnphadengense* resembles *A. nouraguense* and *A. bahnphadengense* but differs from both by having slightly smaller ascospores (6–7 × 2.9–3.7 µm vs 6.2–8.1 × 2.6–3.6 µm for *A. nouraguense* and 6.5–8.5 × 3–3.6 µm for *A. bahnphadengense*) (Fournier & Lechat 2016). Furthermore, *A. nouraguense* exhibits

Fig. 15. *Annulohypoxylon subbahnphadengense* (GMB0469, holotype). **A.** Stromatal habit on wood. **B.** Stromatal surface. **C.** Ostioles and ostiolar discs. **D.** Transverse section of stromata. **E.** Longitudinal section of the stromata showing perithecia. **F–H.** Asci in distilled water. **I.** Stromatal KOH-extractable pigment. **J.** Perispore dehiscent in 10 % KOH. **K.** Ascal apical apparatus (stained in Melzer's reagent). **L–O.** Ascospores. Scale bars: D, E = 0.3 mm; F–H, J–O = 10 µm.

vinaceous grey (116) to vinaceous purple (101) KOH-extractable pigments and slightly smaller perithecia (0.6–0.7 mm diam.) with a larger ostiolar disc (0.3–0.4 mm) (Fournier & Lechat 2016). *Annulohypoxylon bahnphadengense* has stromata with purplish brown tone on the surface, dark vinaceous (82) between perithecial mounds, and smaller perithecia (0.5–0.6 mm diam.) (Fournier *et al*. 2010).

Annulohypoxylon subyungense K. Habib & Q.R. Li, ***sp. nov.*** MB 855598. Fig. 16.

Etymology: Refers to the closely related species *A. yungense*.

Sexual morph: *Stromata* on the surface of the dead branches of unidentified plant, effused-pulvinate, glomerate, hemispherical, surface dark chestnut (40) to fuscous black (105), with olivaceous tones; with perithecial mounds 1/4 exposed, 0.5–2.2 cm long, 0.3–1.6 cm wide, 0.6–0.85 mm high ($\bar{x}$ = 0.9 cm × 0.45 cm × 0.75 mm, *n* = 10), tissue below the perithecial layer black; with 10 % KOH extractable pigments dull green (70). *Perithecia* 410–433 µm high ($\bar{x}$ = 490 × 413 µm, *n* = 20), spherical, 420–590 µm wide, ostioles conical papillate, encircled with a truncatum-type disc, 0.25–0.35 mm diam. *Asci* 95–130 × 5–6.8 µm ($\bar{x}$ = 111 × 6 µm, *n* = 30), 8-spored, unitunicate, cylindrical, long-stipitate, the stipes 30–55 µm long ($\bar{x}$ = 35 µm, *n* = 30), the spore-bearing parts 65–78 µm long ($\bar{x}$ = 70 µm, *n* = 30), with apical apparatus bluing in Melzer's reagent, discoid, 0.8–1.3 × 1.3–1.6 µm (1 × 1.5 µm, *n* = 20). *Ascospores* 8–9.5 × 4–5 µm ($\bar{x}$ = 8.6 × 4.5 µm, *n* = 30), uniseriate, unicellular, inequilateral ellipsoid, with narrowly rounded ends, brown, with inconspicuous straight germ slit covering the full spore length on the convex side, perispore dehiscent in 10 % KOH, smooth with a thickening on the convex side, epispore smooth. *Asexual morph* not observed.

Culture characteristics: Colonies on OA reaching the edge of the Petri dish 5 cm in 3 wk, surface white to pale grey (123), cotton-like, flocculent, rounded, dense; reverse violaceous black (114) or leaden grey (112). Not sporulating on OA nor on PDA.

Secondary metabolites: Stromata contain truncatone A, stygin, and related congeners as major metabolites according to the MS/MS analysis.

Typus: **China**, Yunnan Province, Chuxiong City, Great Montenegro, 23°37'50.24"N, 100°3'33.48"E, subtropical forest, on dead branches, 11 Sep. 2021, *Y.H. Pi*, 2021DHS6 (**holotype** GMB0226, ex-type culture GMBC0226; **isotype** KUN-HKAS 129525).

Barcodes: ITS = PQ278787, LSU = PQ278833, *rpb2* = PQ273663, *TUB2* = PQ273698.

Additional materials examined: **China**, Yunnan Province, Lincang City, Wulao Mountain National Forest Park, 23°85'55.94"N, 100°29'15.25"E, subtropical forest, on dead wood, 9 Aug. 2020, *Y.H. Pi*, 2021WLS16 (**paratype** GMB0228); Yunnan Province, Chuxiong City, Great Montenegro, 23°37'50.24"N, 100°3'33.48"E, subtropical forest, on dead branches, 11 Sep. 2021, *Y.H. Pi*, 2021DHS4 (GMB0482, culture GMBC0482).

Notes: Morphologically and phylogenetically, *A. subyungense* is closely related to *A. yungense*, sharing nearly identical traits. Morphologically, *A. yungense* differs in having a brown vinaceous (84) to black surface colour with red vinaceous tones in mature stromata, larger perithecia (0.4–0.7 mm diam.), long-stipitate asci (43–72 µm), and perithecial mounds that are 2/3 exposed (Kuhnert *et al*. 2017). Furthermore, *A. yungense* yields olivaceous grey (121) to dark brick (60) pigmentation in KOH, whereas the new taxon displays dull green (70) KOH-extractable pigments. The sequence analysis of both species of the ITS and *TUB2* loci showed similarities of 95.9 % and 97.4 %, respectively.

In terms of KOH pigmentation and morphology, *A. subyungense* resembles *A. truncatum*. However, *A. truncatum* differs in having larger ascospores (9–12 × 4–6 µm), larger ostiolar discs (0.2–0.4 mm diam.), and a smaller asci apical apparatus (0.5–1 × 1.5–2 µm). Moreover, the stromatal surface of *A. truncatum* is typically dark brown with reddish tones (Kuhnert *et al.* 2017).

Annulohypoxylon terebratum (J. Fourn. & M. Stadler) Q.R. Li & M. Stadler, ***comb. nov.*** MB 855595.
Basionym: *Rostrohypoxylon terebratum* J. Fourn. & M. Stadler, *Fungal Diversity* **40**: 24. 2010.

Description: See Fournier *et al*. (2010).

Notes: Phylogenetically, *Annulohypoxylon* formed a large clade in the phylogram (Fig. 1). However, the presence of *R. terebratum* (now *A. terebratum)* in the basal branch renders its status polyphyletic. The genus *Rostrohypoxylon* was distinguished from *Annulohypoxylon* by having high conical ostiolate perithecia without a disc, asci without an apical apparatus, and cylindrical ascospores with broadly rounded ends (Fournier *et al.* 2010). In this study, we identified and described *A. coniforme*, which exhibits conical ostiolate perithecia without a disc and is also phylogenetically close to *R. terebratum.* However, most characteristics of our taxon are congruent with *Annulohypoxylon*, except for the conical ostiolate perithecia without disc. Our phylogenetic analysis demonstrates a well-supported sister relationship between *R. terebratum* and *A. coniforme*, further supporting the need for a comprehensive reassessment of the taxonomic status of *Rostrohypoxylon.* In addition, the absence of prominent secondary metabolites in the stromata of *A. coniforme* and *Rostrohypoxylon* limits their comparison with other *Annulohypoxylon* species. Despite this, our metabolomics analysis clusters these species with a high correlation to others in the genus, which are devoid of a specific chemotype. Based on our phylogenies and on morphological considerations, we do not accept *Rostrohypoxylon* as a distinct genus but argue for its inclusion within *Annulohypoxylon*.

Annulohypoxylon thailandicum Daranag. & K.D. Hyde, *Fungal Diversity* **72**: 53. 2015. MB 550799. Fig. 17.

Sexual morph: *Stromata* on the surface of dead branches of unidentified plant, glomerate, spherical, with perithecial mounds conspicuous to 1/4 exposed, or covered by light green tissue; surface black, carbonaceous, 0.2–0.6 cm long, 0.2–0.7 cm wide, 1.5–2 mm thick ($\bar{x}$ = 0.48 cm × 0.56 cm × 1.8 mm, *n* = 10), tissue black between perithecia; with 10 %

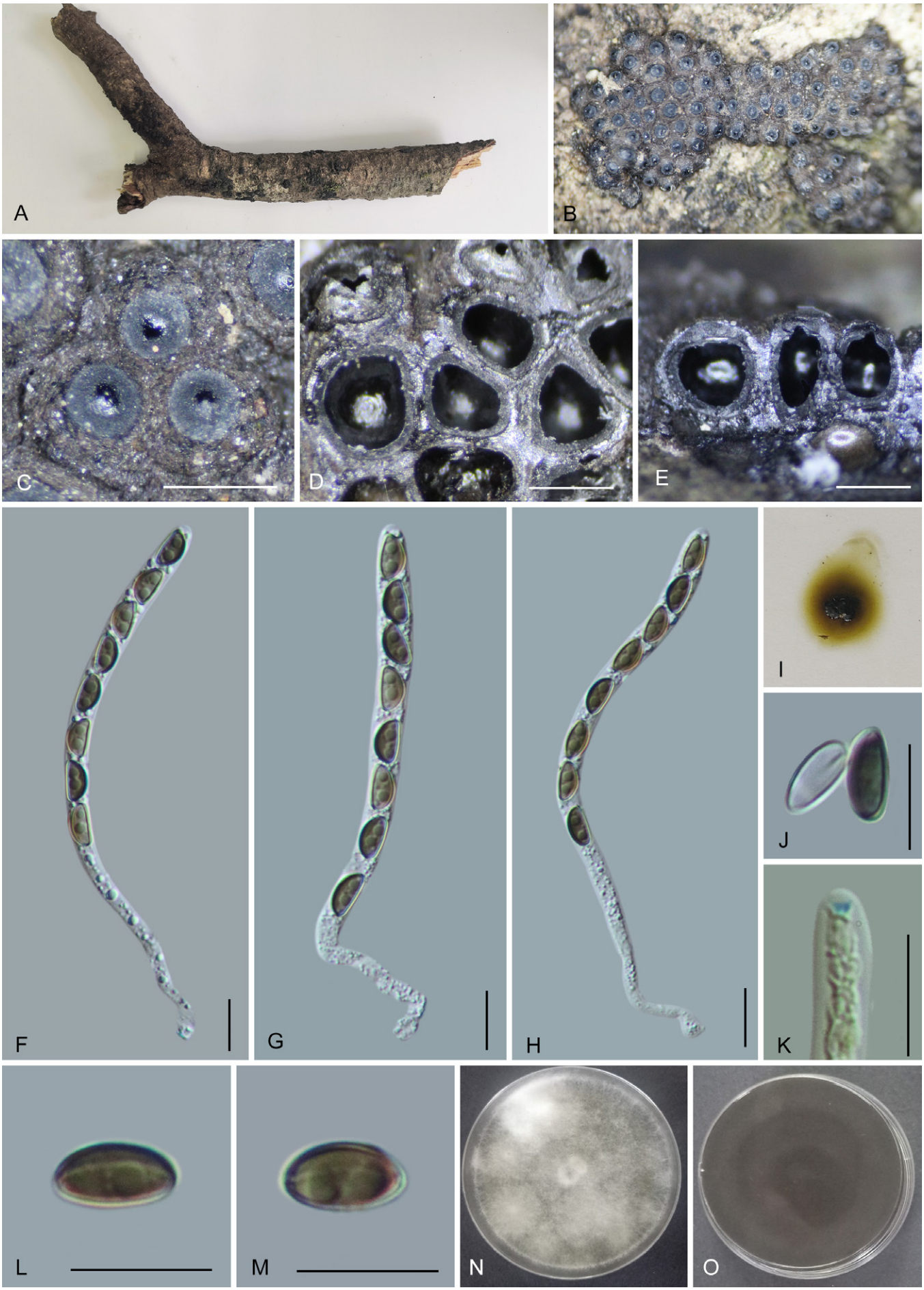

Fig. 16. *Annulohypoxylon subyungense* (GMB0226, holotype). **A.** Stromatal habit on wood. **B.** Stromatal surface. **C.** Ostioles and ostiolar discs. **D.** Transverse section of stromata showing perithecia. **E.** Longitudinal section of the stromata showing perithecia. **F–H.** Asci in distilled water. **I.** Stromatal KOH-extractable pigment. **J.** Perispore dehiscent in 10 % KOH. **K.** Ascal apical apparatus (stained in Melzer's reagent). **L, M.** Ascospores. **N, O.** Colonies on OA (N-upper, O-lower). Scale bars: C–E = 0.5 mm; F–H, J–M = 10 µm.

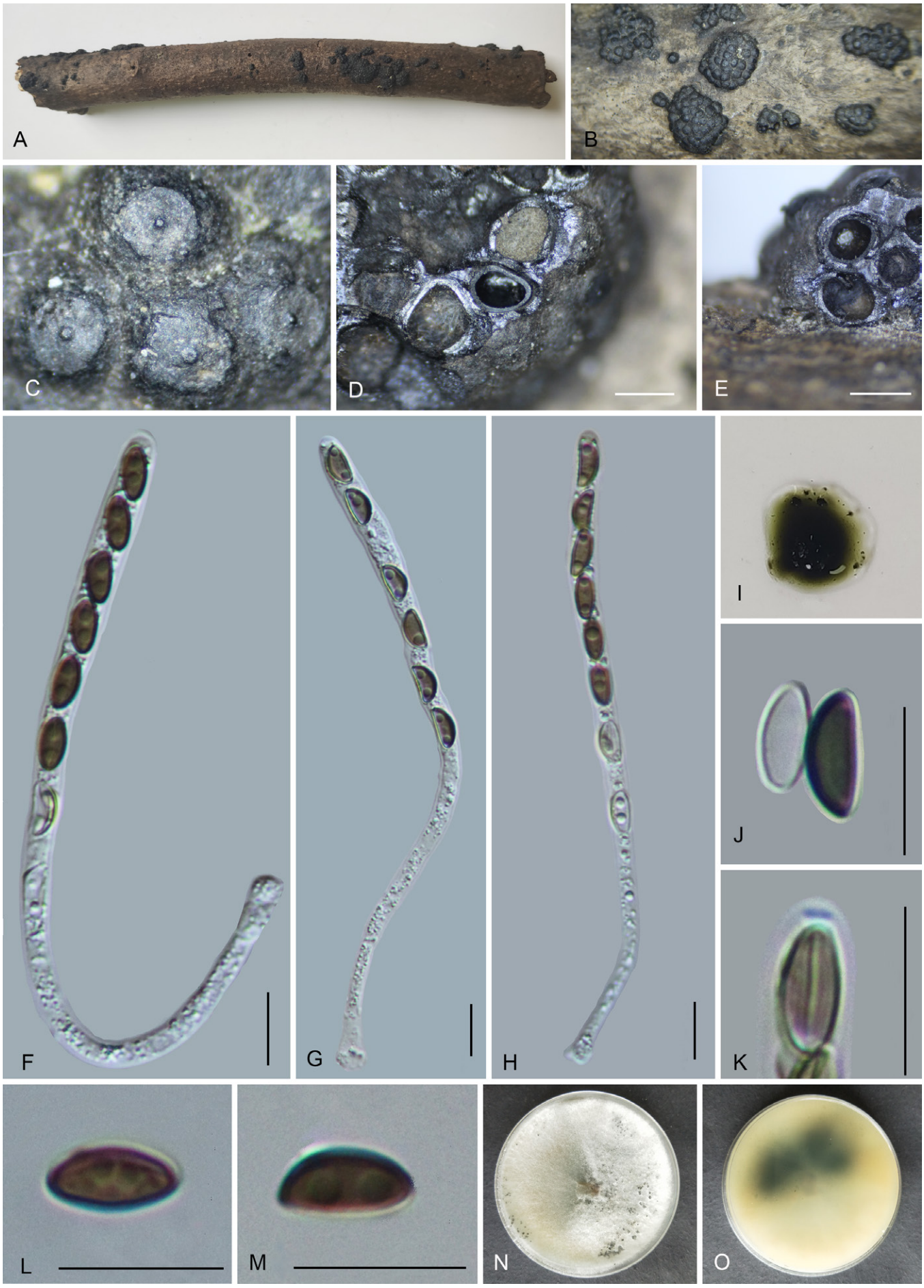

Fig. 17. *Annulohypoxylon thailandicum* (GMB0239). **A.** Stromatal habit on wood. **B.** Stromatal surface. **C.** Ostioles and ostiolar discs. **D.** Longitudinal section of the stromata showing perithecia. **E.** Transverse section of stromata showing perithecia. **F–H.** Asci in distilled water. **I.** Stromatal KOH-extractable pigment. **J.** Perispore dehiscent in 10 % KOH. **K.** Ascal apical apparatus (stained in Melzer's reagent). **L, M.** Ascospores. **N, O.** Colonies on OA (N-upper, O-lower). Scale bars: D, E = 0.5 mm; F–H, J–M = 10 µm.

KOH extractable pigments olivaceous green (90). *Perithecia* 460–566 µm wide, 480–600 µm high ($\bar{x}$ = 510 × 550 µm, *n* = 20), spherical, ostioles conical, papillate, encircled with a truncatum-type disc, 0.3–0.4 mm diam. *Asci* 100–136 × 5–7.5 µm ($\bar{x}$ = 113 × 5.9 µm, *n* = 30), 8-spored, unitunicate, cylindrical, long-stipitate, the stipes 45–70 µm long ($\bar{x}$ = 57 µm, *n* = 30), the spore-bearing parts 60–70 µm long ($\bar{x}$ = 65 µm, *n* = 30), apical apparatus bluing in Melzer's reagent, 1.3–1.8 × 0.5–0.8 µm ($\bar{x}$ = 1.5 × 0.6 µm, *n* = 30). *Ascospores* 7–10 × 3.3–4.5 µm ($\bar{x}$ = 8.5 × 4 µm, *n* = 30), uniseriate, unicellular, inequilateral ellipsoidal with narrowly rounded ends, brown, with conspicuous straight germ slit covering the full spore length on the convex side, perispore dehiscent in 10 % KOH, smooth with a thickening on the convex side, epispore smooth. *Asexual morph* not observed.

Culture characteristics: Colonies on OA reaching the edge of the Petri dish 5 cm in 2 wk, azonate, colonies white, margins diffuse; reverse at first whitish, turning dark cyan blue (27) to slate blue (96). No conidia were observed.

Secondary metabolites: Stromata contain truncatone A, truncatone C, and stygin according to the MS/MS analysis.

Materials examined: **China**, Guizhou Province, Libo County, Maolan Nature Reserve, 25°18'2.76"N, 108°4'29.48"E, subtropical forest, on dead wood of unknown plant, 9 Jul. 2021, *Y.H. Pi*, 2021MLB56 (GMB0239, culture GMBC0239, KUN-HKAS 129521); Hainan Province, Tongguling Nature Reserve, 19°39'38.81"N, 111°0'50.82"E, subtropical forest, on dead wood of unknown plant, 9 Jul. 2020, *Y.H. Pi*, 2020TGL12 (GMB0480, culture GMBC0480, KUN-HKAS 129522); Hainan Province, Tongguling Nature Reserve, 19°39'44.55" N, 111°0'50.03"E, subtropical forest, on dead wood of unknown plant, 9 Jul. 2020, *Y.H. Pi*, 2020TGL32 (GMB0481, culture GMBC0481).

Notes: In the phylogram (Fig. 2), sequences from our collection clustered with those of *A. thailandicum*. Comparative morpho-anatomical analysis also aligns with the description of *A. thailandicum*. Morphologically, *A. thailandicum* resembles *A. archeri*; however, the latter is distinguished by conspicuous perithecial mounds with reddish tones and small spherical perithecia (0.3–0.4 mm diam.) with up to 0.15 mm diam. ostiolar discs (Liu *et al.* 2015, Kuhnert *et al*. 2017). This study reports it as a new record for China.

Annulohypoxylon viridipigmentum Y.H. Pi, K. Habib & Q.R. Li, ***sp. nov.*** MB 855599. Fig. 18.

Etymology: Refers to the green pigments in 10 % KOH.

Sexual morph: *Stromata* on the surface of the dead bark of unidentified plant, effused-pulvinate, with perithecial mounds conspicuous to 1/3 exposed, surface black, carbonaceous, 1–5 cm long, 0.2–0.8 cm wide, 0.9–1.2 mm thick ($\bar{x}$ = 3.6 cm × 0.62 cm × 1 mm, *n* = 10), tissue black between perithecia; with 10 % KOH extractable pigments dull green (70). *Perithecia* 490–535 µm wide, 430–520 µm high ($\bar{x}$ = 507 × 510 µm, *n* = 20), spherical, ostioles papillate, conical, black, encircled with a truncatum-type disc, 0.30–0.38 mm diam. *Asci* 125–140 × 5–6.5 µm ($\bar{x}$ = 132 × 5.5 µm, *n* = 30), 8-spored, unitunicate, cylindrical, long-stipitate, the stipes 45–70 µm long ($\bar{x}$ = 65 µm, *n* = 30), the spore-bearing parts 70–88 µm long ($\bar{x}$ = 75 µm, *n* = 30), apical apparatus not bluing in Melzer's reagent. *Ascospores* 7–9 × 3–4.5 µm ($\bar{x}$ = 8 × 4.3 µm, *n* = 30), uniseriate, unicellular, inequilateral ellipsoidal with rounded ends, brown, with straight germ slit covering the full spore length on the convex side, perispore dehiscent in 10 % KOH, smooth with a thickening on the convex side, epispore smooth. *Asexual morph* not observed.

Culture characteristics: Colonies on OA reaching 5 cm in 2 wk, azonate, at first surface whitish, cottony, after 4 wk, colonies reaching the edge of the 9 cm Petri dish, becoming lavender grey (125), appressed with entire margins, reverse rosy vinaceous (58). No conidia were observed.

Secondary metabolites: Stromata contain truncatone A, stygin, and related congeners as major metabolites according to the MS/MS analysis.

Typus: **China**, Yunnan Province, Jinghong City, Xishuangbannan Nature Reserve, 22°17'35.40"N, 100°55'57.17"E, subtropical forest, on dead bark of unknown plant, 8 Aug. 2021, *Y.H. Pi*, 2021XSBN32 (**holotype** GMB0225, ex-type culture GMBC0225; **isotype** KUN-HKAS 129506).

Barcodes: ITS = PQ278784, LSU = PQ278830, *rpb2* = PQ273660, *TUB2* = PQ273695.

Additional materials examined: **China**, Yunnan Province, Dali City, Tianchi National Nature Reserve (25°52'56.94"N, 99°21'10.25"E), subtropical forest, on dead wood, 4 Aug. 2021, *Y.H. Pi*, 2021TCS230 (**paratype** GMB0465, culture GMBC0465).

Notes: In the BLAST search, *A. viridipigmentum* was found to be more closely related to *A. areolatum*, and also clustered closely with it in phylogenetic analyses. However, *A. areolatum* can be easily differentiated by having smaller stromata (1–5.5 mm diam.), usually containing only up to 10 perithecia (vs 1–5 cm long × 0.2–0.8 cm wide contains frequent perithecia in *A. viridipigmentum*), larger ostiolar discs (0.3–0.7 mm diam. vs 0.30–0.38 mm), stromata surface colour ranging from sepia (116) to grey olivaceous (107) (vs black), and has larger asci 121–181 µm in total length (vs 125–140 × 5–6.5 µm) (Kuhnert *et al*. 2017).

Phylogenetically, it forms a sister relationship with the new species *A. rongjiangense*. Morphologically, they also closely resemble each other, but *A. rongjiangense* differs in having slightly wider ascospores (3.3–5.5 µm) that are almost equilateral ellipsoidal with broadly rounded ends, smaller asci (95–120 × 5.5–8 µm) with shorter stipes (30–45 µm), and a discoid apical apparatus that turns blue in Melzer's reagent. Sequence comparison of the *TUB2* gene between the two species revealed 97 % similarity.

Annulohypoxylon yunnanense Y.H. Pi, K. Habib & Q.R. Li, ***sp. nov.*** MB 855600. Fig. 19.

Etymology: Refers to the locality of type specimen, Yunnan province.

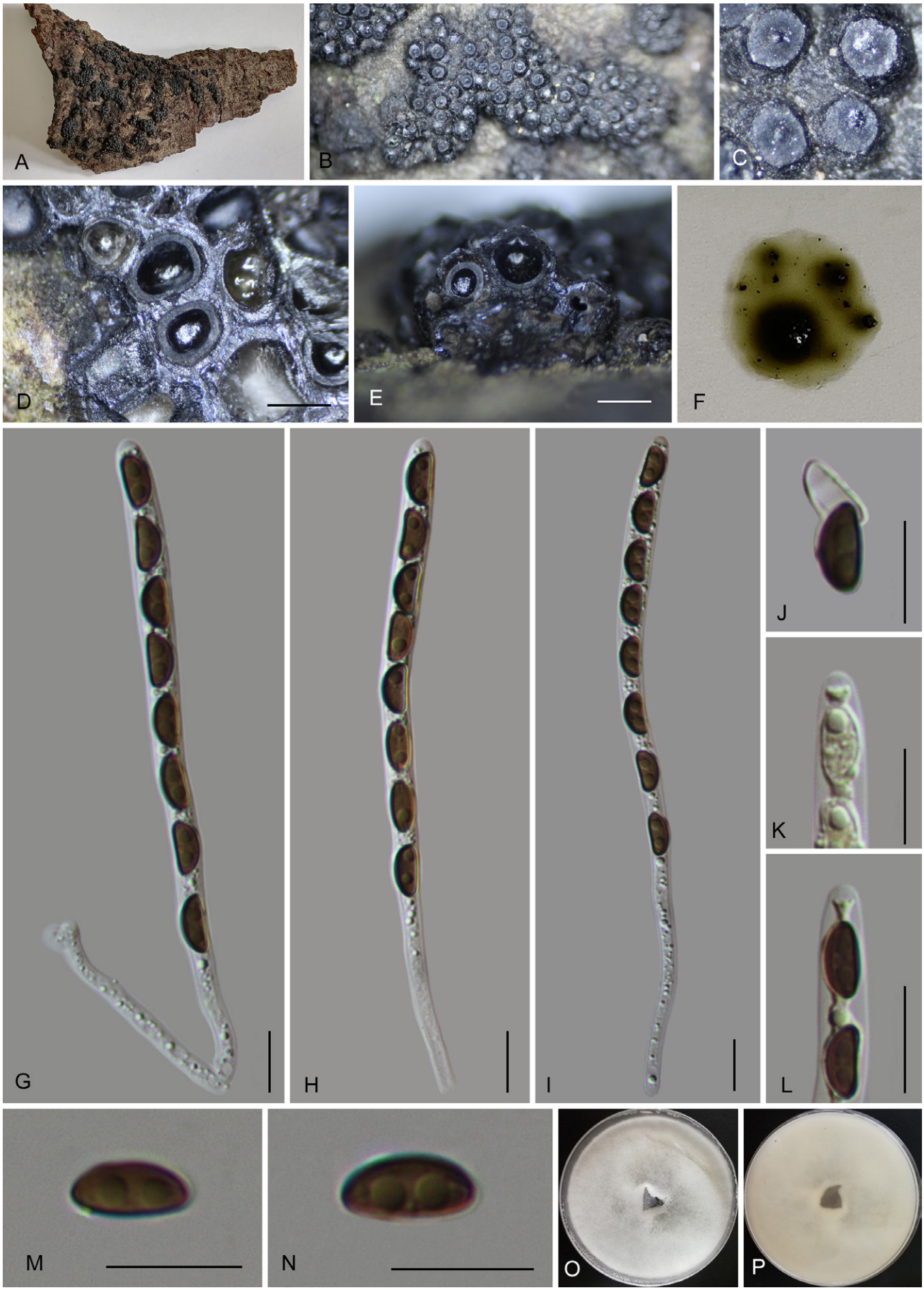

Fig. 18. *Annulohypoxylon viridipigmentum* (GMB0225, holotype). **A.** Stromatal habit on wood. **B.** Stromatal surface. **C.** Ostioles and ostiolar discs. **D.** Transverse section of stroma showing perithecia. **E.** Longitudinal section of the stromata showing perithecia. **F.** Stromatal KOH-extractable pigment. **G–I.** Asci in distilled water. **J.** Perispore dehiscent in 10 % KOH. **K, L.** Ascal apical apparatus (not bluing in Melzer's reagent). **M, N.** Ascospores. **O, P.** Colonies on OA (O-upper, P-lower). Scale bars: D, E = 0.5 mm; G–N = 10 µm.

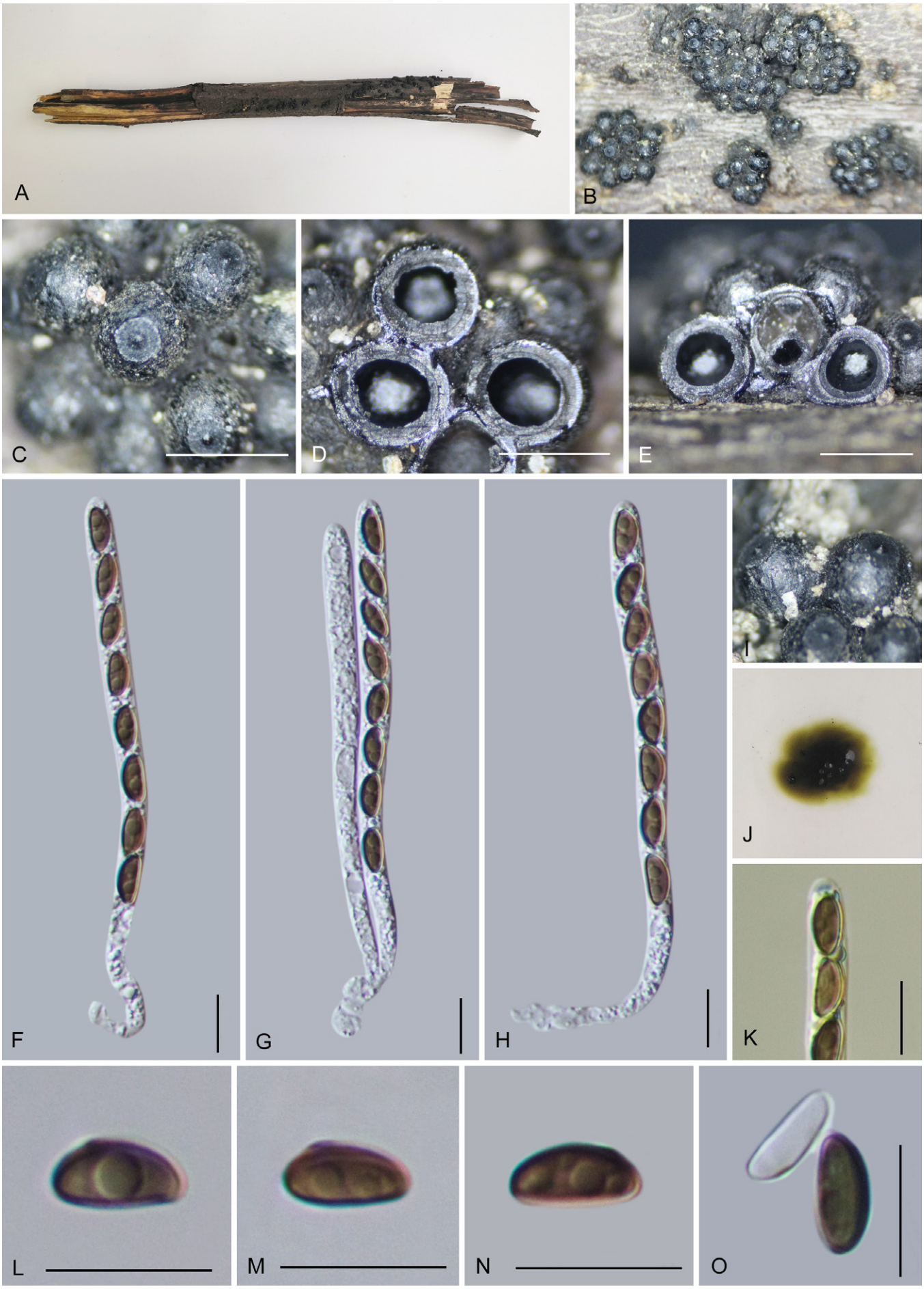

Fig. 19. *Annulohypoxylon yunnanense* (GMB0462, holotype). **A.** Stromatal habit on wood. **B.** Stromatal surface. **C.** Ostioles and ostiolar discs. **D.** Transverse section of stromata. **E.** Longitudinal section of the stromata showing perithecia. **F–H.** Asci in distilled water. **I.** Sharp conical ostioles. **J.** Stromatal KOH-extractable pigment. **K.** Ascal apical apparatus (stained in Melzer's reagent). **L–N.** Ascospores. **O.** Ascospore and perispore dehiscent in 10 % KOH. Scale bars: C–E = 0.5 mm; F–H = 10 µm; K–O = 5 µm.

Sexual morph: *Stromata* on the surface of dead wood, effused-pulvinate, glomerate, hemispherical, slightly constricted at base, surface black, with perithecial mounds up to 1/2 exposed, carbonaceous, 5–12 cm long, 2–5 cm wide, 0.8–1 mm high ($\bar{x}$ = 8 cm × 3.5 cm × 0.9 mm, *n* = 10), tissue below the perithecial layer black; with 10 % KOH extractable pigments olivaceous black (108), grey olivaceous (107); dull green (70). *Perithecia* 365–420 µm wide, 382–453 µm high ($\bar{x}$ = 410 × 409 µm, *n* = 20), spherical, ostioles conical papillate, encircled with a truncatum-type disc, 0.28–0.33 mm diam. *Asci* 91–114 × 5–6.3 µm ($\bar{x}$ = 102 × 5.7 µm, *n* = 30), 8-spored, unitunicate, cylindrical, short-stipitate, the stipes 25–39 µm long ($\bar{x}$ = 32 µm, *n* = 30), the spore-bearing parts 70–75 µm long ($\bar{x}$ = 73 µm, *n* = 30), with apical apparatus bluing in Melzer's reagent, discoid, 1.7–2.4 × 0.7–1.2 µm ($\bar{x}$ = 2 × 0.9 µm, *n* = 20). *Ascospores* 8–10 × 3.5–4.5 µm ($\bar{x}$ = 9.4 × 4.3 µm, *n* = 30), uniseriate, unicellular, inequilateral ellipsoid, with rounded ends, brown, with conspicuous straight germ slit covering the full spore length on the convex side, perispore dehiscent in 10 % KOH, smooth and thickening on the convex side, epispore smooth. *Asexual morph* not observed.

Culture characteristics: Colonies on OA reaching the edge of the Petri dish 5 cm in 3 wk, azonate, surface white to lavender grey (125), felty, cottony, flocculent, with diffuse margins, with scattered black patches; reverse ochreous (44) to isabelline (65). Not sporulating on OA nor on PDA.

Secondary metabolites: Stromata contain truncatone A, stygin, and related congeners as major metabolites according to the MS/MS analysis.

Typus: **China**, Yunnan Province, Baoshan City, Wayao Town, 25°32'14.15"N, 99°28'50.98"E, subtropical forest, on dead wood, 3 Aug. 2021, *Y.H. Pi*, 2021WYZ3 (**holotype** GMB0462, ex-type culture GMBC0462; **isotype** KUN-HKAS 129528).

Barcodes: ITS = PQ278779, LSU = PQ278825, *rpb2* = PQ273655, *TUB2* = PQ273690.

Additional materials examined: **China**, Guizhou Province, Guiyang City, Back Hill of Guizhou Medical University, 26°22'53.00"N, 106°37'40.77"E, subtropical climate, on dead wood, 27 Jun. 2021, *Y.H. Pi*, 2021G3 (**paratype** GMB0464).

Notes: In the BLAST search, *Annulohypoxylon yunnanense* was found to be more closely related to *A. areolatum*, and phylogenetically also appears as sister species. However, *A. areolatum* can be easily differentiated by having smaller stromata (1–5.5 mm diam.), usually containing only up to 10 perithecia, larger ostiolar discs (0.3–0.7 mm diam. vs 0.33–0.38 mm), stromata surface colour ranging from sepia (116) to grey olivaceous (107), and larger asci 121–181 µm in total length (Kuhnert *et al*. 2017). From its stromatal habit and ascospore size, it appears similar to *A. violaceopigmentum*, which also has effused-applanate to effused-pulvinate stromata but the latter has surface vinaceous purple (101), becoming blackish with vinaceous to vinaceous brown tones, large perithecia (0.46–0.6 mm diam.) and yields violet (32) KOH-extractable pigments. Its stromata could be confused with *A. subnitens*, but the latter has larger perithecia (0.6–0.7 mm diam.) and ascospores (7–7.7 × 2.6–3.2 µm) (Fournier & Lechat 2016).

Chemotaxonomic studies

Building upon the findings from Kuhnert *et al.* (2017), herein we have examined 25 *Annulohypoxylon* specimens collected in China by ultrahigh performance liquid chromatography coupled to diode array detection and ion mobility tandem mass spectrometry (UHPLC-DAD-IM-MS/MS). Previously, eight genus-specific chemotypes were defined within *Annulohypoxylon*. However, under the current taxonomic concept of the *Hypoxylaceae*, *Annulohypoxylon* has been segregated from *Jackrogersella*, which contains species known to produce cohaerin- and multiformin-like azaphilones. Therefore, the metabolites found in the stromata of different *Annulohypoxylon* spp. are now mainly classified into two groups: naphthol derivatives, including binaphthalene-tetrols, truncatones, daldinols, and amino acid derived molecules, such as truncaquinones.

We aimed to establish correlations between the taxonomical and chemical distances of the studied specimens by grouping all detected MS features using a hierarchical clustering approach (HCA) (Fig. 21). Our HCA revealed that certain chemotypes represented closely related species, such as *A. bahnphadengense*, *A. subbahnphadengense*, *A. cyclobalanopsidis-glaucae*, *A. maolanense*, *A. limushanense*, and *A. olivaceogriseum* (Clade 1), and *A. rongjiangense*, *A. subyungense*, *A. viridipigmentum*, and *A. yunnanense* (Clade 2). However, some species, despite belonging to different taxonomic subgroups, were devoid of a specific chemotype and were grouped together. This was the case for *A. coniforme* (Clade 4), *A. chuxiongense* (Clade 2), *A. liboense* (Clade 1), *A. microdiscum* (Clade 4), *A. primevalense* (Clade 1), *A. pseudoalbidiscum* (Clade 2), *A. subyungense* (Clade 2), and *A. thailandicum* (Clade 1).

The first chemotype enclosed *A. rongjiangense*, *A. subyungense*, *A. viridipigmentum*, and *A. yunnanense*, all of which belong to clade 2 in our DNA phylogenetic analysis. These species exhibited truncatone A (*m/z* = 319.0965; $C_{20}H_{14}O_4$), stygin (*m/z* = 333.0758; $C_{20}H_{14}O_6$) and related congeners as major metabolites, identified through in silico dereplication. The second group comprised species belonging to different clades (AN1, AN2, and AN4). Specimens clustered together with *A. chuxiongense* presented truncatone A (*m/z* = 319.0965; $C_{20}H_{14}O_4$) and C (*m/z* = 315.0656; $C_{20}H_{12}O_5$) as the major metabolites. *Annulohypoxylon coniforme* did not exhibit prominent secondary metabolites, but shared with *A. liboense* and *A. primevalense* some fatty acid-like molecules. The latter two species exhibited a similar chemotype with several yet unknown azaphilone like-compounds, as suggested by comparison of their MS/MS and UV/Vis spectra with compounds from our in-house library. On the other hand, *A. microdiscum* and *A. pseudoalbidiscum* presented similar metabolite profiles, presenting different so far unknown metabolites in common. Truncatone A (*m/z* = 319.0965; $C_{20}H_{14}O_4$) and hypoxylonol C/F (*m/z* = 319.0965; $C_{20}H_{14}O_4$) were also major metabolites in the stromatal extract of *A. pseudoalbidiscum*.

The third group contains specimens from the clade AN1 such as *A. limushanense*, *A. maolanense*, and *A. olivaceogriseum*. In our analysis, these species presented truncatone A (*m/z* = 319.0965; $C_{20}H_{14}O_4$), truncatone C (*m/z* = 315.0656; $C_{20}H_{12}O_5$), and stygin (*m/z* = 333.0758; $C_{20}H_{14}O_6$) as major metabolites. The closely related species

A. cyclobalanopsidis-glaucae presented a rather unique chemotype from which hypoxylonol C/F (*m/z* = 319.0964; $C_{20}H_{16}O_5$) and related molecules were putatively annotated as major derivatives. The final group enclosed only *A. bahnphadengense* and *A. subbahnphadengense* from the clade AN1. The stromatal extracts from these species presented the most unique/diverse secondary metabolite profiles, including several unknown metabolites. However, some of their major metabolites were identified as truncatone A (*m/z* = 319.0965; $C_{20}H_{14}O_4$) and hinnulin A (*m/z* = 331.0602; $C_{20}H_{12}O_6$).

Dichotomous key to the species reported in this study

1a. Stromatal KOH-extractable pigments other than olivaceous or green 2
1a. Stromatal KOH-extractable pigments olivaceous or green..... 6

2a. Perithecia without ostiolar disc ..... *A. coniforme*
2b. Perithecia with ostiolar disc 3

3a. Ostiolar disc 0.14–0.17 mm diam. ..... *A. microdiscum*
3b. Ostiolar disc > 0.17 mm..... 4

4a. Ascospores with germ slit on the flattened side..... *A. cyclobalanopsidis-glaucae*
4b. Ascospores with germ slit on the convex side 5

5a. Stromata surface black with purplish brown tone on surface, dark vinaceous (82) between perithecial mounds, perithecia 500–600 µm diam. ..... *A. bahnphadengense*
5b. Stromata surface completely black, perithecia 500–800 µm diam. ..... *A. subbahnphadengense*

6a. Ascospore germ slit on the flattened side..... 7
6b. Ascospore germ slit on the convex side 9

7a. Ostiole with a white disc, disc 0.13–0.18 mm diam. ..... *A. limushanense*
7b. Ostiole with a black disc 8

8a. Asci with non-amyloid apical apparatus, ostiolar disc 0.15–0.2 mm diam. ..... *A. maolanense*
8b. Asci with amyloid apical apparatus, ostiolar disc 0.2–0.3 mm diam. ..... *A. olivaceogriseum*

9a. Asci with amyloid apical apparatus..... 10
9b. Asci with non-amyloid apical apparatus..... 15

10a. Asci up to 115 µm in length..... 11
10b. Asci > 115 µm in length 13

11a. Ostiolar disc 0.12–0.15 mm diam. ..... *A. pseudoalbidiscum*
11b. Ostiolar disc > 2 mm diam. 12

12a. Perithecia 365–420 µm wide, ascospores 8–10 × 3.5–4.5 µm ..... *A. yunnanense*
12b. Perithecia 180–350 µm wide, ascospores 6–8 × 2.5–3.5 µm ..... *A. primevalense*

13a. Stromatal surface dark chestnut (40) to fuscous black (105), with olivaceous tones, ostiolar disc 0.25–0.35 mm diam. ..... *A. subyungense*
13b. Stromatal surface black..... 14

14a. Stromata glomerate, ostiolar disc 0.3–0.4 mm diam., asci 100–136 µm in length ..... *A. thailandicum*
14b. Stromata effused-applanate, ostiolar disc 0.35–0.5 mm diam., asci 130–155 µm in length ..... *A. liboense*

15a. Ascospore slightly inequilateral to almost equilateral, ostiolar disc 0.25–0.35 mm diam., asci 95–120 µm in length ..... *A. rongjiangense*
15b. Ascospore inequilateral 16

16a. Perithecia 475–630 µm wide, ostiolar disc 0.35–0.45 mm diam. ..... *A. chuxiongense*
16b. Perithecia 490–535 µm wide, ostiolar disc 0.30–0.38 mm diam. ..... *A. viridipigmentum*

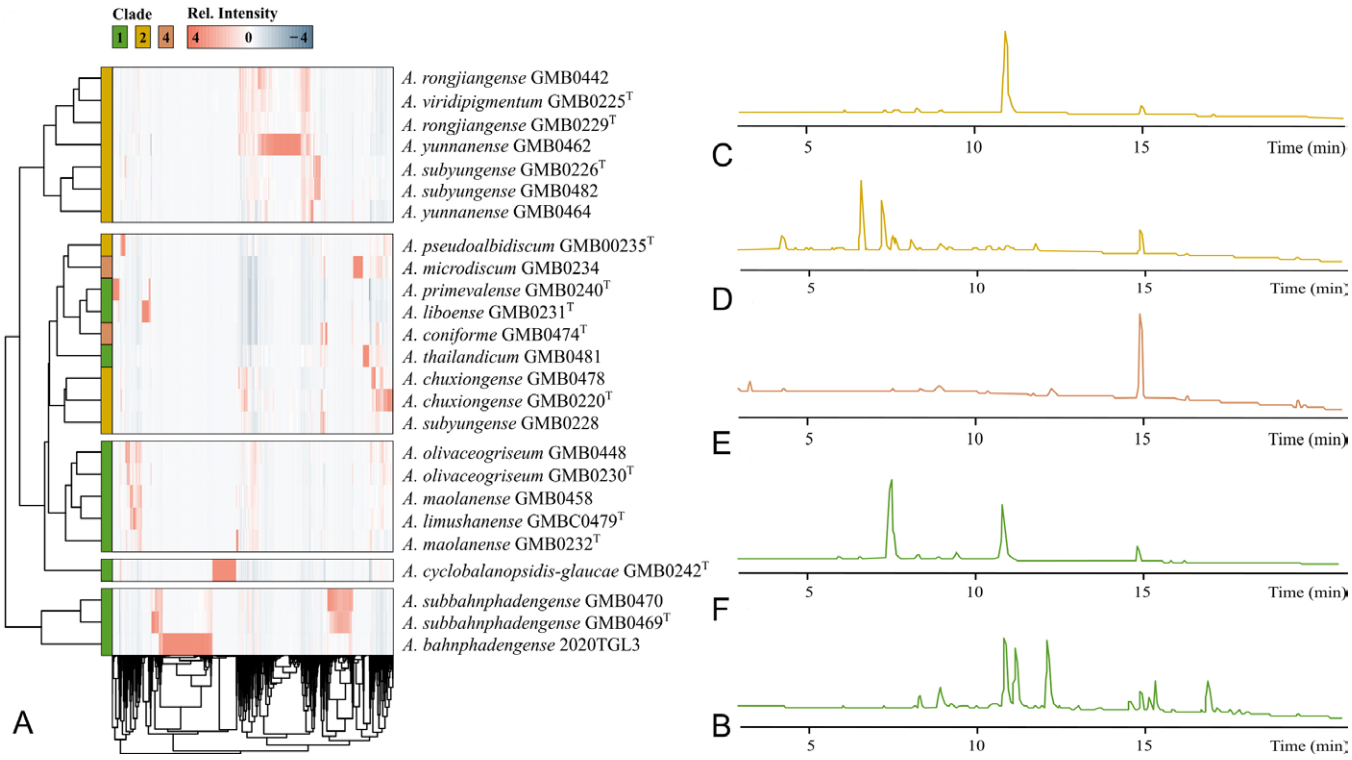

Fig. 20. A. Heatmap following a hierarchical clustering of MS features detected in the stromatal extracts of the studied specimens. Heatmap displays compound abundance values with hierarchical clustering of features and stromatal extracts. Scaled abundance is color-coded from red (high abundance) to dark blue (low abundance). The heatmap with dendrograms was generated by the R package pheatmap. HPLC-UV/Vis chromatograms (210 nm) of the stromatal extracts from representative specimens. **B.** *Annulohypoxylon rongjiangense* GMB0229T. **C.** *A. pseudoalbidiscum* GMB00235T. **D.** *A. microdiscum* GMB0234. **E.** *A. maolanense* GMB0232T. **F.** *A. subbahnphadengense* GMB0469T.

DISCUSSION

The identification of species within the genus *Annulohypoxylon* poses significant challenges due to the limited number of reliable morphological characteristics and the variability in stromatal morphology. For instance, Fournier & Lechat (2016) emphasized the difficulty in distinguishing *Annulohypoxylon* species due to the lack of consistent morphological features. However, they suggested that the morphology of ostiolar discs could serve as a reliable differential character, with the diameter of these discs showing consistency within species. Fournier & Lechat (2016) further highlighted the importance of observing the type of dehiscence of the disc, whether bovei- or truncatum-type, as well as the colour of KOH-extractable pigments and the outermost stromatal coating, which can provide valuable information at the species level. Ascospores are considered significant when they exhibit specific traits such as being pale or dark brown, strongly inequilateral, averaging less than 6 µm long or more than 10 µm long, having a short germ slit, or possessing a perispore that does not dehisce in 10 % KOH solution. Stromatal thickness and perithecial shape and dimensions were highlighted as additional morphological features that may provide information for species differentiation within *Annulohypoxylon*. In our analysis, we found that the length of the asci stipe also provides valuable information for species differentiation within *Annulohypoxylon.* The variation in ascal morphology has already been reported for *Hypoxylon* by Ju & Rogers (1996), who noted that some species differ in the length of their ascal stipes. *Annulohypoxylon limushanense* and *A. pseudoalbidiscum* exhibit very short ascal stipes (ca 15–40 µm), whereas most other species, such as *A. thailandicum*, *A. bahnphadengense*, and *A. viridipigmentum* have longer stipes. In general, it must, however, also be stated that the above studies neither included molecular nor chemotaxonomic data, which are now regarded as state of the art in the taxonomy of the *Hypoxylaceae*.

Kuhnert *et al*. (2017) documented that some ITS sequences of *Annulohypoxylon* species exhibit higher similarity with respective *Hypoxylon* sequences than with other members of *Annulohypoxylon* (e.g. *A. purpureopigmentum*), making barcoding based on ITS challenging. Several studies have highlighted that the utility of ITS sequences in resolving infrageneric relationships within *Annulohypoxylon* is inappropriate due to its polyphyletic nature, particularly when closely related genera like *Hypoxylon* are included in phylogenetic reconstructions (Hsieh *et al.* 2005, Kuhnert *et al.* 2014, 2017, Cedeño-Sanchez *et al.* 2024). The *TUB2* sequences have proven to be a reliable tool for assessing phylogenetic relationships within the *Hypoxylaceae*. Recently, CedeñoSanchez *et al*. (2024) proposed *TUB2* as the primary barcoding marker for *Hypoxylaceae* and other *Xylariales*. Based on the combination of the aforementioned morphological characters, metabolomics analyses, and ITS, LSU, *rpb2* and *TUB2* sequence analysis, investigations in China have unveiled the presence of 17 distinct species of *Annulohypoxylon*. This notable finding includes the identification of 14 previously undescribed species.

Approximately 60 species of *Annulohypoxylon* have been reported worldwide (Wijayawardene *et al.* 2022). Li & Guo (2019) documented the presence of 26 species of *Annulohypoxylon* in China. With two more additions in recent years, totalling 28 species, and including the 17 species reported in this paper, the total number of recognized

Annulohypoxylon species in China now stands at 45. Additionally, the results of our metabolomics profiling suggest a hidden diversity within the stromatal metabolites of the studied specimens. This shows that the biosynthetic potential of these fungi is not fully captured by the so far known metabolites in the genus. Even the mycelial cultures of this genus, which are often isolated as endophytes, constantly yield new metabolites and are most probably widely unexplored (Becker & Stadler 2021). More comprehensive studies are necessary to gain insights into their chemical diversity and provide further insights into their ecological roles and evolutionary relationships.

ACKNOWLEDGEMENTS

This research was supported by the National Natural Science Foundation of China (31960005, 32170019 and 32000009); the Guizhou Medical University High Level Talent Launch Fund Project (2023-058); the Funded Research Projects of the State Key Laboratory of Discovery and Utilization of Functional Components in Traditional Chinese Medicine 2025 (GMUSKL-202510); the High-level Innovation Talents of Guizhou [No. GCC (2023)048]; National Natural Science Foundation of China (12132006); the Guizhou Provincial Natural Science Foundation for High-Level Innovative Talents and Teams (2016-5676, 2015-4021). E. Charria-Girón was supported by the HZI POF IV Cooperativity and Creativity Project Call and the DAAD stipend 57694196 Forschungsstipendien für Doktorandinnen und Doktoranden (2024). Funding from the European Union's Horizon 2020 research and innovation program (RISE) under the Marie Skłodowska-Curie grant agreement No. 101008129, project acronym "Mycobiomics" to M.S., S.W. and E.C.G. is also gratefully acknowledged. The authors wish to thank U. Beutling for the metabolomics measurements.

DATA AVAILABILITY

The data sets generated during and/or analysed during the current study are available in the MycoBank repository (included in the manuscript), and GenBank (included in Table 1). Furthermore, the data sets generated during and/or analysed during the current study are available from the corresponding author upon request. The alignment file is provided as supplementary data S1.

Declaration on conflict of interest The authors declare that there is no conflict of interest.

REFERENCES

Altschul SF, Gish W, Miller W, *et al.* (1990). Basic local alignment search tool. *Journal of Molecular Biology* **215**: 403–410. https://doi.org/10.1016/S0022-2836(05)80360-2

Ariyawansa HA, Hyde KD, Jayasiri SC, *et al.* (2015). Fungal diversity notes 111–252: taxonomic and phylogenetic contributions to fungal taxa. *Fungal Diversity* **75**: 27–274. https://doi.org/10.1007/s13225-015-0346-5

Bills GF, Gonzalez-Menendez VMJ, Platas G, *et al.* (2012). *Hypoxylon pulicicidum sp. nov*. (*Ascomycota*, *Xylariales*), a pantropical insecticide-producing endophyte. *PLoS ONE* **7**: e46687. https://doi.org/10.1371/journal.pone.0046687

Bitzer J, Læssøe T, Fournier J, *et al.* (2008). Affinities of *Phylacia* and the daldinoid *Xylariaceae*, inferred from chemotypes of cultures and ribosomal DNA sequences. *Mycological Research* **112**: 251–270. https://doi.org/10.1016/j.mycres.2007.07.004

Cedeño-Sanchez M, Charria-Girón E, Lambert C, *et al.* (2023). Segregation of the genus *Parahypoxylon* (*Hypoxylaceae*, *Xylariales*) from *Hypoxylon* by a polyphasic taxonomic approach. *MycoKeys* **95**: 131–162. https://doi.org/10.3897/mycokeys.95.98125

Cedeño-Sanchez M, Cheng T, Lambert C, *et al.* (2024). Unravelling intragenomic polymorphisms in the high-quality genome of *Hypoxylaceae*: a comprehensive study of the rDNA cistron. *Mycological Progress* **23**: 5. https://doi.org/10.1007/s11557-023-01940-2

Cheng MJ, Wu MD, Chen JJ (2023). Secondary metabolites from the endophytic fungus *Annulohypoxylon stygium* var. *annulatum*. *Chemistry of Natural Compounds* **59**: 1009–1011. https://doi.org/10.1007/s10600-023-04181-7

Cheng MJ, Wu MD, Chen JJ (2012). Secondary metabolites and cytotoxic activities from the endophytic fungus *Annulohypoxylon squamulosum*. *Phytochemistry Letters* **5**: 219–223. https://doi.org/10.1016/j.phytol.2011.12.012

Daranagama DA, Camporesi E, Tian Q, *et al.* (2015). *Anthostomella* is polyphyletic comprising several genera in *Xylariaceae*. *Fungal Diversity* **73**: 203–238. https://doi.org/10.1007/s13225-015-0329-6

Daranagama DA, Liu XZ, Chamung S, *et al.* (2014). A multigene genealogy reveals the phylogenetic position of *Rhopalostroma lekae*. *Phytotaxa* **186**: 177–187. https://doi.org/10.11646/phytotaxa.186.4.1

De Long Q, Liu LL, Zhang X, *et al.* (2019). Contributions to species of *Xylariales* in China-1. *Durotheca* species. *Mycological Progress* **18**: 495–510. https://doi.org/10.1007/s11557-018-1458-6

Dutta G, Singh RK (2023). A checklist of the *Hypoxylaceae* and *Xylariaceae* species of India. *Kavaka* **59**: 68–87. https://doi.org/10.36460/Kavaka/59/3/2023/68-87

Feng J, Surup F, Hauser M, *et al.* (2020). Biosynthesis of oxygenated brasilane terpene glycosides involves a promiscuous N-acetylglucosamine transferase. *Chemical Communications* **56**: 12419–12422. https://doi.org/10.1039/D0CC03950K

Fournier J, Lechat C (2016). Some *Annulohypoxylon* spp. (*Xylariaceae*) from French Guiana, including three new species. *Ascomycete.org* **8**: 33–53. https://doi.org/10.25664/art-0169

Fournier J, Flessa F, Peršoh D, *et al*. (2011). Three new *Xylaria* species from Southwestern Europe. *Mycological Progress* **10**: 33–52. https://doi.org/10.1007/s11557-010-0671-8

Fournier J, Stadler M, Hyde KD, *et al*. (2010). The new genus *Rostrohypoxylon* and two new *Annulohypoxylon* species from Northern Thailand. *Fungal Diversity* **40**: 23–36. https://doi.org/10.1007/s13225-010-0026-4

Franco ME, Wisecaver JH, Arnold AE, *et al.* (2022). Ecological generalism drives hyperdiversity of secondary metabolite gene clusters in xylarialean endophytes. *New Phytologist* **233**: 1317–1330. https://doi.org/10.1111/nph.17873

Gardes M, Bruns TD (1993). ITS primers with enhanced specificity for basidiomycetes – application to the identification of mycorrhizae and rusts. *Molecular Ecology* **2**: 113–118. https://doi.org/10.1111/j.1365-294X.1993.tb00005.x

Gan D, Wang CY, Li CZ, *et al.* (2022). Secondary metabolites from

Annulohypoxylon sp. and structural revision of emericellins A and B. *Journal of Natural Products* **85**: 828–837. https://doi.org/10.1021/acs.jnatprod.1c00922

Glass NL, Donaldson GC (1995). Development of primer sets designed for use with the PCR to amplify conserved genes from filamentous ascomycetes. *Applied and Environmental Microbiology* **61**: 1323–1330.

Hall TA (1999). BioEdit: a user-friendly biological sequence alignment editor and analysis program for Windows 95/98/NT. *Nucleic Acids Symposium Series* **41**: 95–98.

Hladki AI, Romero AI (2009). Taxonomic and nomenclatural aspects of *Hypoxylon* taxa from southern South America proposed by Spegazzini. *Mycologia* **101**: 733–744. https://doi.org/10.3852/09-020

Hsieh HM, Ju YM, Rogers JD (2005). Molecular phylogeny of *Hypoxylon* and closely related genera. *Mycologia* **97**: 844–865. https://doi.org/10.1080/15572536.2006.11832776

Hyde KD, Norphanphoun C, Maharachchikumbura SSN, *et al.* (2020). Refined families of *Sordariomycetes*. *Mycosphere* **11**: 305–1059. https://doi.org/10.5943/mycosphere/11/1/7

Hyde KD, Noorabadi MT, Thiyagaraja V, *et al.* (2024). The 2024 Outline of Fungi and fungus-like taxa. *Mycosphere* **15**(1): 5146–6239. https://doi.org/10.5943/mycosphere/15/1/25

Ikeda A, Matsuoka S, Masuya H, *et al.* (2014). Comparison of the diversity, composition, and host recurrence of xylariaceous endophytes in subtropical, cool temperate, and subboreal regions in Japan. *Population Ecology* **56**: 289–300. https://doi.org/10.1007/s10144-013-0412-3

Ju YM, Rogers JD (1996). A revision of the genus *Hypoxylon*. American Phytopathological Society Press.

Ju YM, Rogers JD, Hsieh HM (2004). New *Hypoxylon* species and notes on some names associated with or related to *Hypoxylon*. *Mycologia* **96**(1): 154–161.

Katoh K, Rozewicki J, Yamada KD (2019). MAFFT online service: multiple sequence alignment, interactive sequence choice and visualization. *Briefings in Bioinformatics* **20**: 1160–1166. https://doi.org/10.1093/bib/bbx108

Koukol O, Kelnarová I, Černý K (2015). Recent observations of sooty bark disease of sycamore maple in Prague (Czech Republic) and the phylogenetic placement of *Cryptostroma corticale*. *Forest Pathology* **45**: 21–27. https://doi.org/10.1111/efp.12129

Kuhnert E, Fournier J, Peršoh D, *et al.* (2014). New *Hypoxylon* species from Martinique and new evidence on the molecular phylogeny of *Hypoxylon* based on ITS rDNA and β-tubulin data. *Fungal Diversity* **64**: 181–203. https://doi.org/10.1007/s13225-013-0264-3

Kuhnert E, Sir EB, Lambert C, *et al.* (2017). Phylogenetic and chemotaxonomic resolution of the genus *Annulohypoxylon* (*Xylariaceae*) including four new species. *Fungal Diversity* **85**: 1–43. https://doi.org/10.1007/s13225-016-0377-6

Lambert C, Wendt L, Hladki AI, *et al.* (2019). *Hypomontagnella* (*Hypoxylaceae*): A new genus segregated from *Hypoxylon* by a polyphasic taxonomic approach. *Mycological Progress* **18**: 187–201. https://doi.org/10.1007/s11557-018-1452-z

Lee D, Hwang BS, Choi P, *et al.* (2019). Hypoxylonol F isolated from *Annulohypoxylon annulatum* improves insulin secretion by regulating pancreatic β-cell metabolism. *Biomolecules* **9**(8): 335. https://doi.org/10.3390/biom9080335

Li W, Guo L (2019). *Annulohypoxylon bawanglingense*, *A. diaoluoshanense*, *A. guangxiense*, and *A. sichuanense spp. nov*. and new records from China. *Mycotaxon* **134**(3): 431–438. https://doi.org/10.5248/134.431

Liu YL, Whelen S, Hall BD (1999). Phylogenetic relationships among ascomycetes: Evidence from an RNA polymerse II subunit. *Molecular Biology and Evolution* **16**: 1799–1808. https://doi.org/10.1093/oxfordjournals.molbev.a026092

Liu Y, Kurtan T, Mandi A, *et al.* (2018). A novel 10-membered macrocyclic lactone from the mangrove-derived endophytic fungus *Annulohypoxylon* sp. *Tetrahedron Letters* **59**(7): 632–636. https://doi.org/10.1016/j.tetlet.2018.01.001

Maciel OMC, Tavares RSN, Caluz DRE, *et al.* (2018). Photoprotective potential of metabolites isolated from algae-associated fungi *Annulohypoxylon stygium*. *Journal of Photochemistry and Photobiology B: Biology* **178**: 316–322. https://doi.org/10.1016/j.jphotobiol.2017.11.018

Miller MA, Pfeiffer W, Schwartz T (2010). Creating the CIPRES Science Gateway for inference of large phylogenetic trees. 2010 Gateway Computing Environments Workshop (GCE), New Orleans, Louisiana, 14 Nov 2010. IEEE, New York: 1–8.

O'Donnell K, Cigelnik E (1997). Two divergent intragenomic rDNA ITS2 types within a monophyletic lineage of the fungus *Fusarium* are nonorthologous. *Molecular Phylogenetics and Evolution* **7**: 103–116. https://doi.org/10.1006/mpev.1996.0376

Quang DN, Hashimoto T, Nomura Y, *et al.* (2005). Cohaerins A and B, azaphilones from the fungus *Hypoxylon cohaerens*, and comparison of HPLC-based metabolite profiles in *Hypoxylon* sect. Annulata. *Phytochemistry* **66**: 797–809. https://doi.org/10.1016/j.phytochem.2005.02.006

Rambaut A (2012). *FigTree: Tree Figure drawing tool 2006–2012*, version 1.4.0. Institute Evolutionary Biology, University Edinburgh.

Rayner RW (1970). *A mycological colour chart*. Kew and British Mycological Society, Commonwealth Mycological Institute, Kew.

Ronquist F, Teslenko M, Van Der Mark P, *et al.* (2012). MrBayes 3.2: Efficient Bayesian phylogenetic inference and model choice across a large model space. *Systematic Biology* **61**: 539–542. https://doi.org/10.1093/sysbio/sys029

Samarakoon MC, Hyde KD, Maharachchikumbura SS, *et al.* (2022). Taxonomy, phylogeny, molecular dating and ancestral state reconstruction of *Xylariomycetidae* (*Sordariomycetes*). *Fungal Diversity* **112**(1): 1–88. https://doi.org/10.1007/s13225-021-00495-5

Senanayake IC, Rathnayaka AR, Marasinghe DS, *et al.* (2020). Morphological approaches in studying fungi: Collection, examination, isolation, sporulation and preservation. *Mycosphere* **11**(1): 2678–2754. https://doi.org/10.5943/mycosphere/11/1/20

Sir EB, Becker K, Lambert C, *et al.* (2019). Observations on Texas hypoxylons, including two new *Hypoxylon* species and widespread environmental isolates of the *H. croceum* complex identified by a polyphasic approach. *Mycologia* **111**(4): 1–25. https://doi.org/10.1080/00275514.2019.1637705

Sir EB, Kuhnert E, Hladki AI, Romero AI (2018). *Annulohypoxylon* (*Hypoxylaceae*) species from Argentina. *Darwiniana* **6**(1): 68–83. https://doi.org/10.14522/darwiniana.2018.61.777

Sir EB, Kuhnert E, Surup F, *et al.* (2015). Discovery of new mitorubrin derivatives from *Hypoxylon fulvo-sulphureum sp. nov*. (*Ascomycota*, *Xylariales*). *Mycological Progress* **14**: 28. https://doi.org/10.1007/s11557-015-1043-1

Sir EB, Kuhnert E, Surup F, *et al.* (2016). New species and reports of *Hypoxylon* from Argentina recognized by a polyphasic approach. *Mycological Progress* **15**: 42. https://doi.org/10.1007/s11557-016-1182-z

Stadler M, Kuhnert E, Peršoh D, *et al.* (2013). The *Xylariaceae* as model examples for a unified nomenclature following the "One

Fungus-One Name" (1F1N) concept. *Mycology* **4**(1): 5–21. https://doi.org/10.1080/21501203.2013.782478

Stadler M, Læssøe T, Fournier J, *et al.* (2014). A polyphasic taxonomy of *Daldinia* (*Xylariaceae*). *Studies in Mycology* **77**: 1–143. https://doi.org/10.3114/sim0016

Stamatakis A (2014). RAxML Version 8: A tool for phylogenetic analysis and post-analysis of large phylogenies. Bioinformatics **30**(9): 1312–1313. https://doi.org/10.1093/bioinformatics/btu033

Tang AMC, Jeewon R, Hyde KD (2009). A re-evaluation of the evolutionary relationships within the *Xylariaceae* based on ribosomal and protein-coding gene sequences. *Fungal Diversity* **34**(1): 127–155. https://doi.org/10.1007/s13225-009-0007-2

Triebel D, Peršoh D, Wollweber H, *et al.* (2005). Phylogenetic relationships among *Daldinia*, *Entonaema*, and *Hypoxylon* as inferred from ITS nrDNA sequences. *Nova Hedwigia* **80**: 25–43. https://doi.org/10.1127/0029-5035/2005/0080-0025

Wendt L, Sir EB, Kuhnert E, *et al.* (2018). Resurrection and emendation of the *Hypoxylaceae*, recognized from a multigene phylogeny of the *Xylariales*. *Mycological Progress* **17**(2): 115–154. https://doi.org/10.1007/s11557-017-1311-3

White TJ, Bruns TD, Lee SB, *et al.* (1990). Amplification and direct sequencing of fungal ribosomal RNA genes for phylogenetics. In: *PCR protocols: A guide to methods and applications* (Innis MA, Gelfand DH, Sninsky JJ, *et al.*, eds), Academic Press Inc., London, UK: 315–322. https://doi.org/10.1016/B978-0-12-372180-8.50042-1

Wijayawardene NN, Hyde KD, Dai DQ, *et al.* (2022). Outline of *Fungi* and fungus-like taxa – 2021. *Mycosphere* **13**(1): 53–453. https://doi.org/10.5943/mycosphere/13/1/2

Zhang JF, Liu JK, Hyde KD, *et al.* (2023). Ascomycetes from karst landscapes of Guizhou Province, China. *Fungal Diversity* **122**: 1–160. https://doi.org/10.1007/s13225-023-00524-5

Zhang N, Castlebury LA, Miller AN, *et al.* (2006). An overview of the systematics of the *Sordariomycetes* based on a four-gene phylogeny. *Mycologia* **98**(6): 1076–1087. https://doi.org/10.1080/15572536.2006.11832635

SUPPLEMENTARY MATERIAL

Data S1. Multilocus alignment in FASTA format used to generate the phylogenetic trees.